UNIVERSITY OF THE
WITWATERSRAND,
JOHANNESBURG

Parametric Optimization of the Production of Carbon Nanotube Yarn from CVD Reactor

MSc Research Dissertation

Prepared by

Bodiba Veronica (539766)

Submitted to

School of Chemical and Metallurgical Engineering, Faculty of Engineering and the Built Environment,
University of the Witwatersrand, Johannesburg, South Africa

Supervisor: Prof Michael Daramola

Co-supervisor: Prof Sunny Iyuke

June, 2020

Declaration

I hereby declare that this dissertation is my own work. It is being submitted for the degree of Master of Science in Engineering to the University of the Witwatersrand, Johannesburg, South Africa. It has not been submitted for any degree or examination to any other University.

…… 29/June/2020

Signature of Candidate Day Month Year

Dedication

I would like to thank my family for being my great support system throughout my studies. I would further like to appreciate my supervisors for their guidance and assistance. I would also like to thank University of Johannesburg Physics Department for allowing me to use their equipment. Above all, I would like to thank the almighty God for giving me the strength and the ability to complete my work.

Abstract

Carbon nanotubes (CNTs) have attracted research efforts due to their excellent properties which include; high tensile strength, good thermal and electrical conductivities. To utilize their good properties, CNTs can be further made into strong pure CNT yarns by spinning them. However, the production of macroscale carbon nanotube (CNT) yarns that has similar or excellent properties as microscale CNTs is still a problem. Thus the produced CNT yarns usually have low quality due to defects formed during the production process. This is because CNT bundles tend to slide in yarn microstructures, thus making it difficult to transfer individual CNT properties into spun yarn structure. Furthermore, the amount of CNT yarn produced using CVD method is very small. Therefore, this research will focus on parametric optimization of production parameters for achieving high CNT yarn yield and enhancing CNT yarn properties. The interested parameters include; the reaction temperature, flow rate of carbon precursor (methane) and the state of the catalyst.

Hence it was necessary to optimize the CNT yarn production using CVD reactor with the aim of enhancing the yield and quality. Single-walled carbon nanotubes (SWCNTs) have a higher electrical conductivity as compared to multi-walled carbon nanotubes (MWCNTs) thus the production of SWCNTs is desired. Methane gas was chosen as the carbon precursor for this study because literature states that saturated hydrocarbons produce large amounts of SWCNTs than unsaturated hydrocarbons. Moreover, methane is a natural gas and it is available everywhere in the world, therefore the production process will be very affordable and the usage of methane might decrease global warming. Thus methane gas was used to help obtain more single-walled carbon nanotubes. The parametric variables including reactor temperature, flow rate of carbon precursor and the state of catalyst were manipulated into improving the yield and quality of CNT yarns.

Individual CNTs have excellent properties; however it is difficult to produce CNT yarns with similar properties as individual CNTs. CNT yarns appear to be more of interest to researchers because of their versatility in real life application. With that said; the study contained in this dissertation investigated the parametric optimization for the production of CNT yarn using CVD method.

Carbon nanotube yarns are nano-scale filamentary composites made up of individual CNTs aligned in cross-section that follows helical paths at different angles about the yarn axis. Carbon nanotube yarn properties increases with increasing length and decreasing diameter. Other factors that affect the electrical and mechanical properties of CNT yarns are; densification, water evaporation and CNT orientation. Theory states that mechanical strength is directly proportional to CNT yarn length and is inversely proportional to the CNT yarn diameter. Furthermore, CNT yarn has got excellent mechanical properties and good electrical conductivity too.

The objective of this research was to produce and characterize CNTs and CNT yarn from CVD reactor; and to investigate the effect of operating parameters (reactor temperature, methane flow rate and the effect of dissolving catalyst in liquid hydrocarbons). The production of the CNT yarn was carried out using CVD method in the following four steps: (i) The production of CNTs, (ii) Conversion of CNTs to CNT yarn and (iii) Characterization of the CNT yarn.

The Response Surface Methodology (RSM) was used to develop the empirical equation for predicting the experimental responses and this model was justified using experimental data. The experiments were carried out using a vertical CVD reactor with methane as a precursor and Ferrocene as a catalyst. From the results obtained in this study show that CNT yield is higher when cyclopentane is used to dissolve Ferrocene as compared to the production were solid Ferrocene was used. SEM images have shown better CNT morphology when catalyst state was changed to liquid by dissolving ferrocene in cyclopentane. Moreover, the CNTs produced with liquid state catalyst were more pronounced, free of impurities, more aligned and longer compared to the CNTs produced with solid Ferrocene. The optimal CNTs achieved were produced at 1000ºC using liquid catalyst. The amount of the sample obtained at the optimal conditions was 165 mg and the electical conductivity and the I_D/I_G ratio were 0.2388 mA and 0.16, respectively.

The CNT yarn was then produced with Ferrocene dissolved in cyclopentane since the best results from CNTs production were obtained when using liquid catalyst. CNT yarns were produced at methane flow rate of $160\,ml/min$ and $150\,ml/min$ while varying temperature between $900℃ - 100℃$. CNT yarn yield improved at higher methane flowrate and increased with increasing temperature.

The results from SEM images showed evidence of impurities from the catalyst. The sample's I_D/I_G ratios and electrical conductivity improved with the increasing reaction temperature and worsened with increasing methane flow rate. After completing the optimization study, optimal CNT yarn production was achieved at 967ºC reaction temperature with 150 ml/min methane flow rate. The yield and the electrical conductivity of the CNT yarn synthesized at optimal conditions were found to be 24.72 mg and 0.217 mA, respectively.

Publications from the thesis

1. Mahangani, N., Igbokwe,E., Aberefa, O., Bodiba,V., Daramola, M.O.,Iyuke,S.E. (2019) Production of CNT yarns from methane gas for use as filaments in incandescent bulbs: Thermodynamic properties of as-spun CNT yarns, 2019 J. Phys.: Conf. Ser. 1378 022019 https://doi.org/10.1088/1742-6596/1378/2/022019

2. Bodiba, V., Igbokwe, E., Mahangani, N., Aberefa, O., Daramola, M.O., Iyuke, S.E. (2018) Production of CNT yarns for use as filaments in incandescent bulb: effect of carbon source and state of catalyst on production of CNT, IOP Conf. Ser.: Mater. Sci. Eng. 413, 012027 doi:10.1088/1757-899X/413/1/012027

LIST OF FIGURES

LIST OF TABLES

NOMENCLATURE

CNTs – Carbon Nanotubes

d – CNT Diameter

GPa - Gigapascals

L – CNT Length

SWCNTs – Single-walled Carbon Nanotubes

MWCNTs – Multi-walled Carbon Nanotubes

ºC – Degrees Celsius

mA – Milliamperes

SEM – Scanning Electron Microscopy

EDX – Energy-Dispersive X-ray Spectroscopy

μm - Micrometer

mg – Milligram

H_2 – Hydrogen gas

CH_4 – Methane gas

CHAPTER ONE

1.0. Introduction

Carbon nanotube is defined as a sheet of graphene rolled up in a cylindrical shape and consists of excellent chemical and physical properties (Panth, 2018). Some of the good properties of carbon nanotube include low density, high aspect ratio, high tensile strength and high electrical and thermal conductivities (Jayasinghe et al., 2013) Due to the excellent properties of Carbon nanotubes (CNTs), more opportunities in Nanotechnology have emerged (Panth, 2018).

CNTs can be manufactured using various methods such as plasma method, arch discharge, evaporation method, laser ablation, thermal synthesis and chemical vapour deposition (CVD). The most common employed method for the production of CNTs is chemical vapour deposition mainly due to its simplicity and the capability for mass production (Pandey et al., 2016).

CNTs are available as single-walled and multi-walled commonly known as SWCNTs and MWCNTs, respectively. SWCNTs consist of a single layer of graphene having a diameter between 0.4 – 2 nm. Whereas MWCNTs are made of more than one layer of graphene sheets forming coaxial cylinders with diameters ranging between 4-100 nm (Pandey et al., 2016). Single-walled carbon nanotubes (SWCNTs) have a higher electrical conductivity as compared to multi-walled carbon nanotubes (MWCNTs) for the reason that the larger the diameter the lower the electrical and thermal conductivities (Behabtu et al., 2008). It is currently difficult to achieve SWCNTs only through a CVD reactor since it mostly produces a mixture of SWCNTs and MWCNTs. This has a bad impact on electrical properties because the electrical conductivity of MWCNTs is very low when compared to that of pure SWCNTs. The study done by Choo et al. (2012) states that the latter is caused by the presence of amorphous carbon and other impurities that hinder the flow of electrons (Choo et al., 2012).

Literature states that saturated hydrocarbons produce large amounts of SWCNTs than unsaturated hydrocarbons (Awasthi et al., 2005). Methane gas was then selected as the carbon precursor for this study in an attempt to achieve more SWCNTs than MWCNTs. Methane gas is also a primary component of natural gas and it is one of the abundant greenhouse gases possessing global warming effects that are greater than that of carbon dioxide (Howarth et al., 2011). Methane is also available everywhere in the world which makes the production of CNTs

affordable. Thus using methane gas as carbon precursor will enhance the production of large amount of SWCNTs.

To utilize their good properties, CNTs can be further made into strong pure CNT yarns through spinning. Similarly with CNTs, CNT yarns have unique combination properties including high mechanical strength, electrical and thermal conductivity, electrochemical activity and corrosion resistivity (Miao, 2020). Furthermore, the latter mentioned microscopic properties enables CNT yarns to offer a much wider range of applications such as growing multifunctional fabrics (Luo et al., 2019). However, the production of macro scale carbon nanotube (CNT) yarns that have similar or excellent properties as micro scale CNTs is still a problem (Liu et al., 2010). Often the produced CNT yarns usually have low quality due to defects formed during the production process. According to Choo et al. CNT spun yarns have illustrated poor characteristics when compared to individual CNTs (Choo et al., 2012). This is because CNT bundles tend to slide in yarn microstructures, thus making it difficult to transfer individual CNT properties into spun yarn structure (Jayasinghe et al., 2013). Furthermore, the amount of CNT yarn produced using CVD method is very small. This research focused on the parametric optimization of production parameters for achieving high CNT yarn yield and enhancing CNT yarn properties.

Methods such as array spinning from the CNT forest liquid crystallization, coagulation spinning and surfactant based spinning can be employed to spin CNTs into CNT macrostructures. The common method of spinning CNTs into CNT yarn is direct spinning of aerogel from the gas phase during production of CNT using CVD method (Vilatela et al., 2012). CNT yarns appear to be more of interest to researchers because of their versatility in real life application (Liu et al., 2016).

The proof of concept for the production of CNT yarn has already been demonstrated by various researchers where in some cases CNT yarn electronic properties were harnessed to manufacture nanowires (Vilatela et al., 2012). Preliminary studies on the production of CNT yarn from the swirled floating catalyst chemical vapour deposition (SFCCVD) have also been completed successfully (Aberefa et al., 2018). However, there is still a huge room for improving the quality of the CNT yarn for mass production since the properties of CNT yarns are still very low when compared to individual CNTs (Choo et al., 2012). Therefore, the overall aim of this study is to produce CNT yarn with similar properties to the individual CNTs using CVD method.

1.1.Problem Statement

A CVD method has been and is currently used for the production of CNT yarns. However, the amount of yarn produced is very small (Baughman et al., 2002). In previous research studies, the quality of CNTs was low as compared to the properties of individual CNTs (Jayasinghe et al., 2013; Hayashi et al., 2015). The effect of temperature plays a major role in the production of CNT yarns, because most carbon precursor starts decomposing at higher temperatures and usually this leads to catalyst poisoning by the amorphous carbon present in the reaction which results in low CNT yarn yield (Xiaodong et al., 2005). Other studies have further reported that high concentration of carbon precursors contributes to the amount of amorphous carbon produced and this causes defects in the CNT yarns produced. Consequently, this results in poor quality of the produced CNT yarn (Weissker et al., 2010). Therefore, the overall aim of this study is to produce CNT yarn with similar properties to the Individual CNTs using CVD method and using Research Surface Methodology (RSM) to optimize the CNT yarn production.

1.2.Research Questions, aim and objectives

The research seeks to answer the following questions;

1. Can high quality CNT yarn be produced from CNT in a CVD reactor using methane gas as the carbon precursor?
2. Can the production of CNT yarn from CNT be optimized to result in enhanced quality and yield of the produced CNT yarn?

The study reported in this dissertation aimed at optimizing the production of the CNT yarn from the CVD reactor through improving the quality and yield of CNT yarn. This was achieved using RSM method to derive a mathematical and statistical model for the experimental design.

The following are the research objectives of this dissertation

1. To produce and characterize CNT from CVD method using methane as the feedstock and investigate the effect of operating parameters and state of catalyst
2. To produce and characterize CNT yarn from CVD method using methane as the feedstock and investigate the effect of temperature and state of catalyst

1.3.Expected Outcome

The expected outcomes from this research studies were:

1. The production, characterization and optimization data for CNTs and CNT yarn as a contribution to the existing body of knowledge in the field
2. A well-written dissertation on the findings as a reference document

1.4.Dissertation Outline

Chapter One

The general introduction to the purpose of this study including; problem statement, research questions, research aims and objectives and the expected outcomes are well defined in this section.

Chapter Two

An extensive background on the history and properties of the CNTs and CNT yarn, production methods of CNTs, alternative ways of spinning CNTs into CNT yarn, purification methods of CNT yarn and lastly parametric optimization of CNT yarn are presented in this chapter.

Chapter Three

This chapter meticulously explains the experimental setup, materials and methods used to manufacture CNTs and CNT yarn. The optimization methodology used in this study is also described in this chapter.

Chapter Four

The results from the CNTs and CNT yarn formation are analyzed in this chapter where the morphology of the samples is presented in SEM images. Raman Spectroscopy and Four probe method were used to study the purity and electrical conductivity of the produced samples respectively. The analysis of the results was compared to the past research work done on the CNT and CNT yarn optimization.

Chapter Five

The parametric effect of production variables and optimization study are obtainable in this chapter where the focus of the optimal conditions was based on the yield, the purity and the electrical conductivity of the CNT and CNT yarn.

Chapter Six

The general summary of the completed study is reported in this section which incorporates overall conclusions drawn from the former chapters. Recommendations for future work study are also included in this chapter.

CHAPTER TWO

2.0. Literature review

2.1.Carbon Nanotube Structure

Carbon nanotube is described as a single sheet of graphene rolled up in a cylindrical shape (Panth, 2018). CNTs are known for their unique size, shape and incredible physical properties. The diameter of CNTs does not exceed 100 nm and their width ranges between 1-2 nm. CNTs are considered to be closely one dimensional mainly due to the length to diameter ratio of around 1000 (Aqel et al., 2012). The electronic, thermal and physical properties of CNTs vary greatly depending on the CNT diameter, length, chirality and or twist angle (Scoville et al., n.d).

The SP^2 bonds between carbon nanotube atoms enables CNTs to have a high tensile strength than that of steel and Kevlar. The defects in the structure of CNTs weaken the tensile strength. These defects are either caused by the rearrangement in the carbon bonds or in the atomic vacancies (Scoville et al., n.d). Moreover, the strength between the carbon atoms allows CNTs to withstand high temperatures thus making CNTs good thermal conductors when compared to copper (Hwang et al., 2011; Scoville et al., n.d). The tensile strength of CNTs is around 50-200 GPa according to research (Scoville et al., n.d). CNTs possess approximately 1000 times current density when compared to copper, which is currently the most used conductor in electronic field (Wei et al., 2004).

CNTs can either be rolled into a single sheet or multiple sheets thus forming single-walled nanotubes (SWCNTs) or multi-walled nanotubes (MWCNTs), respectively (Hwang et al., 2011). SWCNTs are made up of single graphene sheet rolled to form a cylinder. MWCNTs are made up of cylindrical arrays of SWCNTs which are formed concentrically (Coleman et al., 2006).

2.1.1.Single-walled Nanotubes

SWCNT is made up from one layer of graphene sheet rolled up in a cylindrical shape. There are three known types of SWCNTs namely; Armchair, Chiral and Zigzag. The type of the SWCNT depends on how the sheet of graphene is rolled. A pair of indices (n,m) are used to define the structure of SWCNT where this indices is called a chiral vector (Aqel et al., 2012). The three types of SWCNT structures are illustrated in Figure 1.

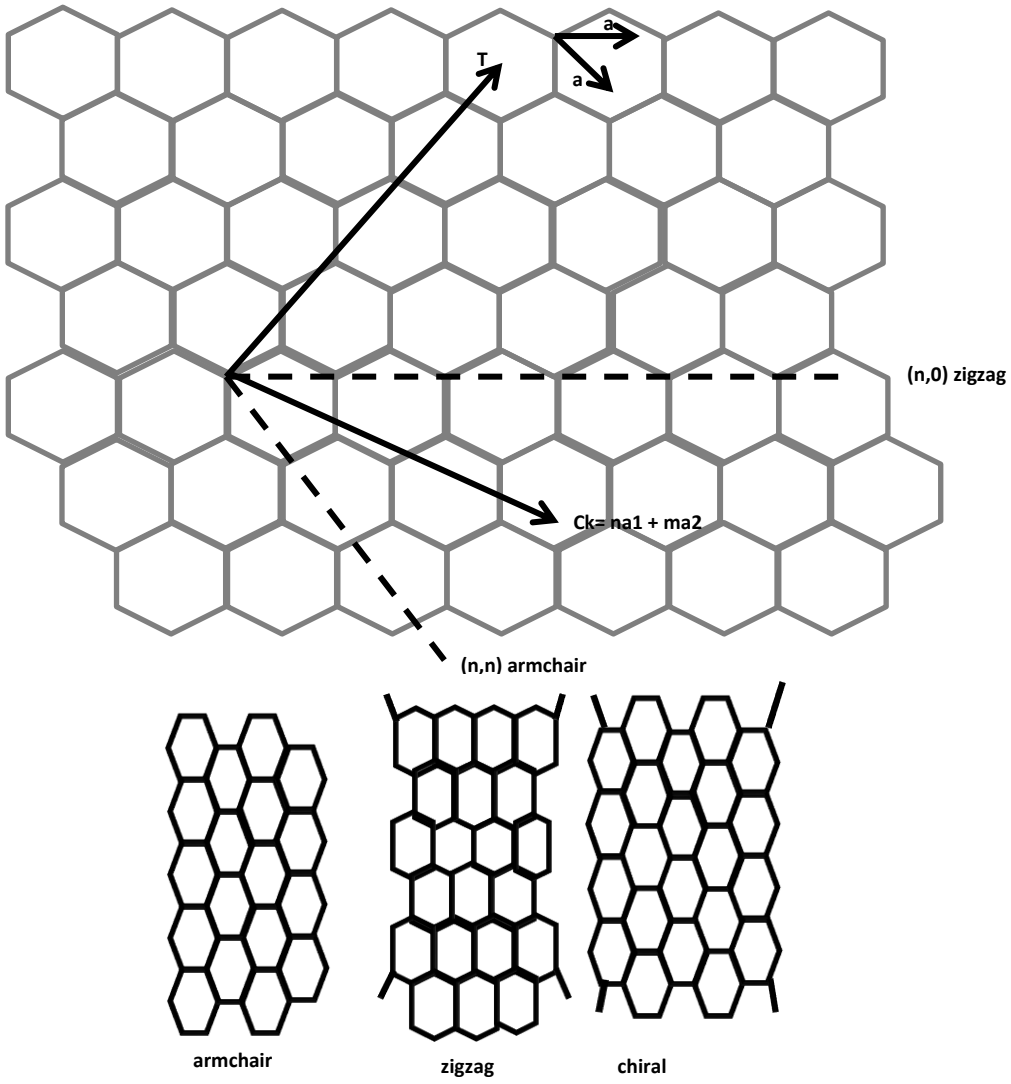

Figure 1: The three types of SWCNTs (Adapted from Panth, 2018)

Electrical properties of SWCNTs differ according to their structures; armchair nanotubes are always metallic and chiral and zigzag structures are semiconducting. The diameter of SWCNT is estimated between 1-10nm. The electrical property of SWCNTs surpasses that of MWCNTs (Scoville et al., n.d). The production of SWCNTs still remains expensive thus making it difficult for large scale production (Aqel et al., 2012).

2.1.2.Multi-walled Nanotubes

On the other hand, MWCNTs have got two structural models known as Russian-doll and Parchment model. The Russian-doll structure is made up of nanotubes with various diameters where the nanotube with a smaller diameter is kept inside the nanotube with a larger diameter. In

the Parchment model the same nanotube graphene is rolled around itself multiple times. Often in MWCNTs, the outer walls prevent a chemical interaction between the inner nanotubes and outside materials from occurring. Research also states that MWCNTs have higher tensile strength than SWCNTs (Scoville et al., n.d). The MWCNT diameter ranges between 5 to few hundreds nm (Hwang et al., 2011).

2.2.Methods of Carbon Nanotube Production

There are various methods of production used to manufacture CNTs. Production methods of shorter CNTs are as follows; arch discharge, laser oven, High pressure CO conversion (HiPco) is cheaper and more scalable because it does not use preformed catalysts), fluidized bed chemical vapor deposition (CVD: cost effective and high production rate of CNTs) or production methods of longer nanotubes (substrate growth CVD, catalytic gas flow) (Szabo et al., 2010). In this research study CVD method will be used.

2.2.1.Laser Ablation

Laser evaporation is a process that produces CNTs by vaporizing a piece of graphite target using laser irradiation at high temperatures in an inert atmosphere (Awasthi et al., 2005). The advantages of laser ablation technique are the high yield of carbon nanotubes and the low metallic impurities that exist in the product. Carbon nanotubes formed using this technique usually contains some branching. This method is expensive (Eatemadi et al., 2014). However this process produces many defects CNTs at lower temperatures. Moreover, high purity rods are required, thus making this process very expensive (Awasthi et al., 2005). Figure 2 depicts a laser ablation process for the production of CNTs, where the laser is focused on the metal loaded graphite rod to vaporize it. Argon is used as an inert gas which is bled into the chamber to carry the carbon from high temperature reactor into the cooled side for the collection. The CNTs form on the cooler side of the reactor as a result of condensation of the vaporized carbon (Chrzanowska et al., 2015).

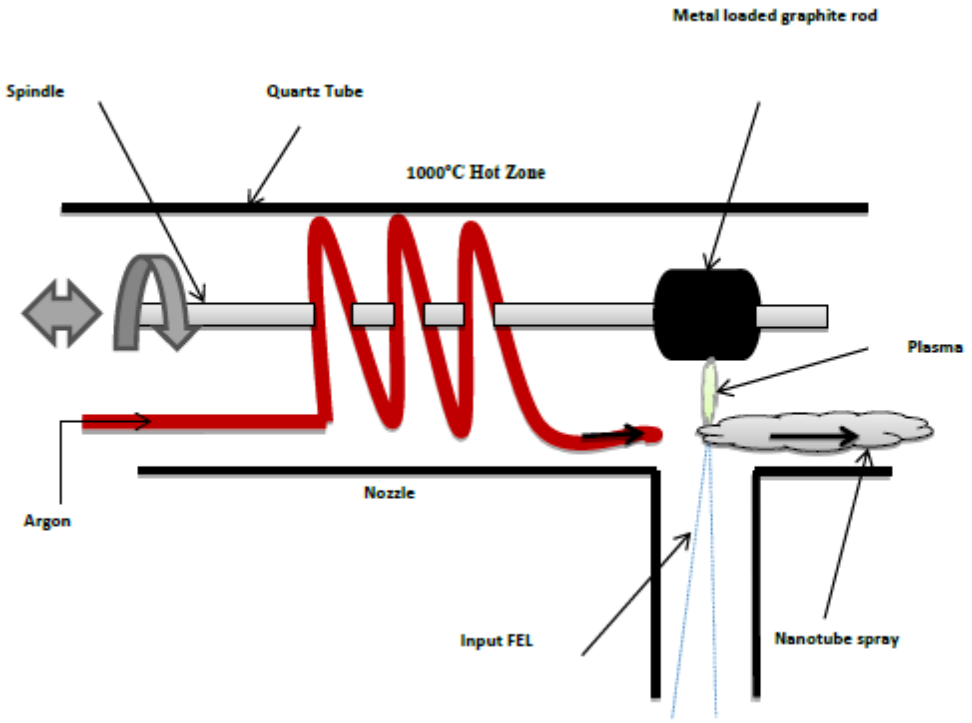

Figure 2: An illustration of laser ablation set-up (adapted from Awasthi et al., 2005)

2.2.2.Arc Discharge Method

Arc discharge was used in early discoveries to produce SWCNTs, now the most common methods for the production of SWCNTs are laser ablation and chemical vapor deposition (CVD). SWCNTs are usually super-conducting, although carbon nanotubes are either semi-conducting or prestine (extremely conductive). It is common for SWCNTs to form bundles because of their high flexibility and great surface energy. This creates a problem because bundle SWCNTs have limited/ poor properties and it is difficult to separate bundles (Coleman et al., 2006). The process of arch discharge uses high temperatures, and this causes CNT to expand leading to less structural defects (Awasthi et al., 2005). This technique produces scalable amount of nanotubes. However it is difficult to control the chirality of the nano fibers formed in this process. Also purification of the products is required (Eatemadi et al., 2014).

Arch discharge can be used for the production of MWCNTs; this result in similar fibers as perfect SWCNTs. MWCNTs yarns formed using arch discharge acts as metals or small bandgap semi-conductors (Coleman et al., 2006). The arc discharge process for CNT production is

depicted in Figure 3, where two graphite rods are used as anode and cathode electrodes. A vacuum pump is used to produce arc plasma between the electrodes. The arc then influences the anode electrode to sublimate while the carbon deposits on the cathode electrode in the form of carbon nanotube and other types of carbon (Sharma et al., 2015).

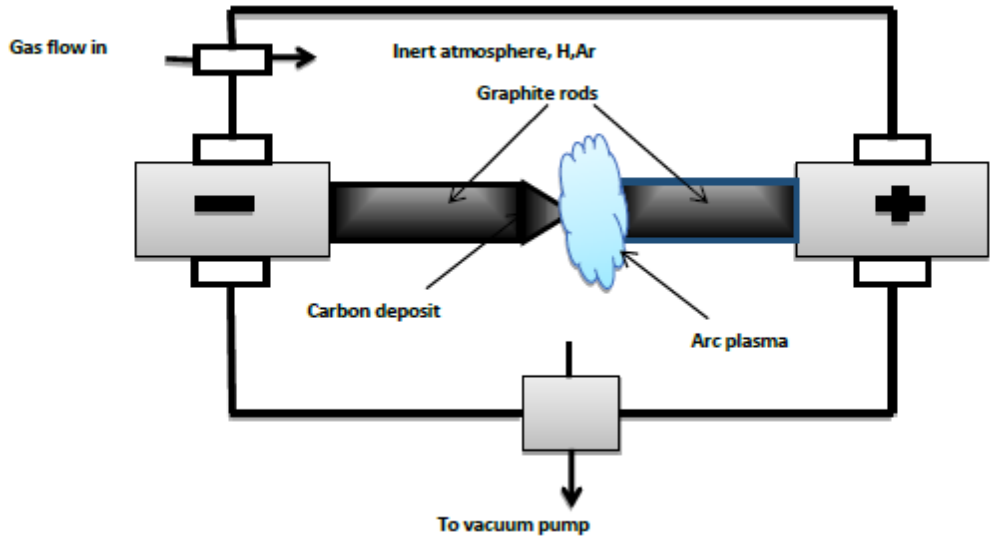

Figure 3: Demonstration of arc discharge method (adapted from Coleman et al., 2006)

2.2.3.Chemical Vapour Deposition

CVD method is favoured because parameters of the nanotubes such as length, diameter, purity, density and alignment can be easily and accurately controlled at low temperatures. Here, hydrocarbons are broken down on a catalyst support or in the presence of floating catalyst through the contact with metallic catalyst particles. High purity nanotubes are produced when using this method and large quantity of CNTs is produced (Eatemadi et al., 2014).

CVD method has got long time reaction and uses medium temperatures ranging between $700 - 1473\ K$. This method enables the production of high quality MWCNTs and SWCNTs onto a substrate or as a raw material. CVD method is favoured because no further purification of

CNT is needed (Awasthi et al., 2005).There are three types of CVD processes and these are; thermal CVD, plasma enhanced CVD and Catalytic CVD (Awasthi et al., 2005).

(i) Thermal CVD

The energy used to produce CNTs in thermal CVD method is driven by the high reactor temperatures. Thermal CVD processes are carried out at atmospheric pressure, where the carbon precursor and inert gas are pumped into the reactor chamber (Dahmen, 2003). Thermal CVD is favoured due to its less construction costs and its simplicity to build. Quartz tube is inserted in the thermal CVD reactor. Thermal CVD allows manipulation of parameters to give high yield. Usually high temperatures between $700-1000\,℃$ are used in thermal CVD method. This however negatively impacts the entire process since some desirable substrate materials such as glass cannot be used due to high temperatures.

In thermal CVD, CNT growth parameters such as deposition rate, crystallinity and density greatly depend on the reaction temperature (Dahmen, 2003). Furthermore, the CNTs produced with thermal CVD method are often not well aligned when compared to CNTs synthesized with plasma enhanced CVD method (Bell et al., 2006). Some of the disadvantages of thermal CVD include; stress formation, higher diffusion rates for elements from the substrate into film and the likelihood of the substrate to degrade (Dahmen, 2003).

Figure 4 illustrates the formation of CNTs using thermal CVD method. Ammonia is used as a carbon precursor, while hydrogen is used as an inert gas. Both gases are injected into the reactor that is kept at high temperature. The substrate with catalyst is placed inside the reactor to from CNTs as the catalyst and gases dissociate (Awasthi et al., 2005).

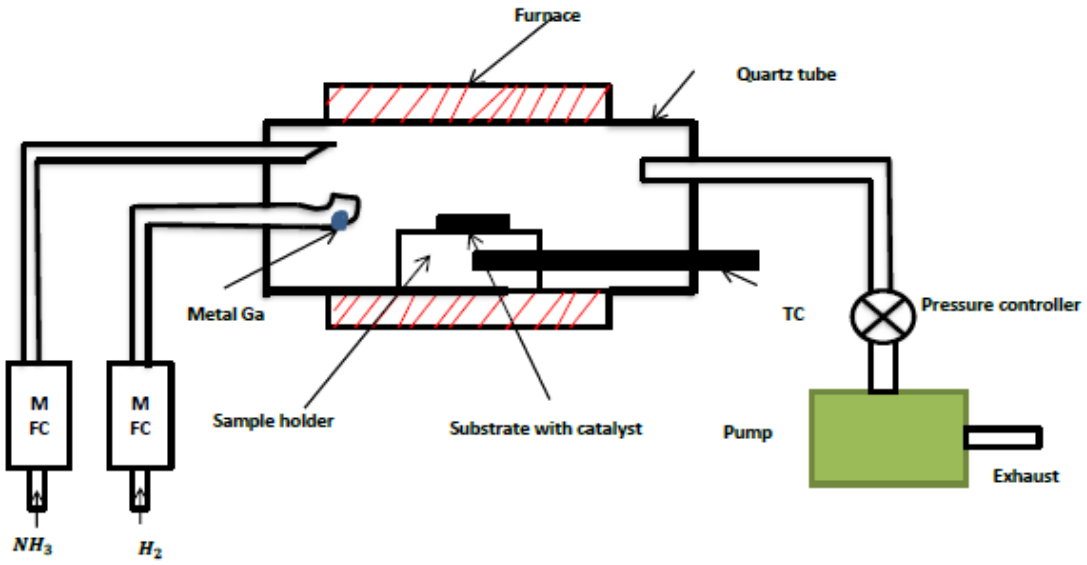

Figure 4: An illustration of a thermal CVD reactor (Adapted from Awasthi et al., 2005)

(ii) Catalytic CVD

This method usually uses a supported catalyst material which is placed inside a furnace. Carbon Nano yarn can be grown as root or tip growth when using the CVD method (Eatemadi et al., 2014). Catalytic chemical vapour deposition (CCVD) is favoured for its high efficiency and low cost method for synthesizing CNTs with high yields and purity. During the process of CCVD, CNTs are produced by the catalytic decomposition of hydrocarbon vapours (Rashid et al., 2015).

Here catalyst particle remains attached at the support surface. The root growth considers the effects of support-particle interaction. The tip growth method occurs as a result of the weak support-catalyst interaction. This happens when the catalyst is detached from the support surface (Eatemadi et al., 2014).

Catalytic pyrolysis produces aligned CNTs bundles in one step and production costs are low. It is stated in theory that less quantity of ferrocene yields large amounts of MWCNTs, whereas SWCNTs are a result of using dilute hydrocarbons-organometallic mixtures (Awasthi et al., 2005)

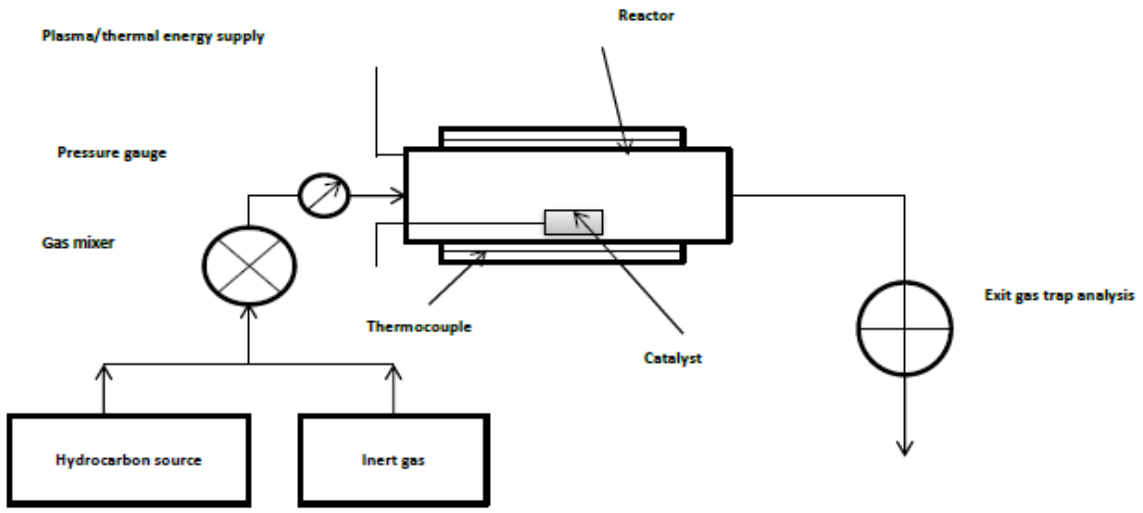

Figure 5: An illustration of catalytic CVD reactor (adapted from Awasthi et al., 2005)

(iii) Plasma-enhanced CVD (PECVD)

Plasma-enhanced CVD (PECVD) uses inert gas plasma to activate the reaction for the deposition of thin films. The use of plasma leads to reduced deposition temperature as compared to thermal CVD method. Carbon deposition can occur at room temperature due to the high energy that is present in the plasma. The plasma consists of partially or ionized gas that is generally a mixture of electrons, charged particles and neutral atoms which create high energy in the plasma. The deposition of thin films in PECVD is influenced by the energy found in the plasma discharge (Vasudev, 2015).

The plasma used in PECVD allows the use of both organic and inorganic carbon sources unlike with the thermal CVD that only uses inorganic precursors (Hamedani, 2015). When using the PECVD method, carbon precursor dissociates in the presence of a plasma and the transition-metal catalyst (Bell et al., 2006). Due to the high energy in the plasma, lower temperatures between $600 - 700℃$ are used for the dissociation of carbon source and nanotube formation. CNTs produced with PECVD are highly aligned and this is due to the presence of the electric field in the plasma (Bell et al., 2006).

The plasma used in PECVD can be formed using various processes such as; radio frequency PECVD, microwave PECVD, inductively coupled PECVD and DC glow discharge PECVD (Bell et al., 2006). Figure 6 below illustrates the PECVD reactor, where a coated substrate with metal is placed onto a heating plate in the centre of the PECVD reactor. The reactor is then pumped to low base pressure to release atmospheric gasses. Inert gasses are pumped into the reactor and the high voltage applied forms the plasma. CNTs are then formed by the dissociation of gases due to the energy from heating the substrate and from the high voltage plasma (Schumacher, nd).

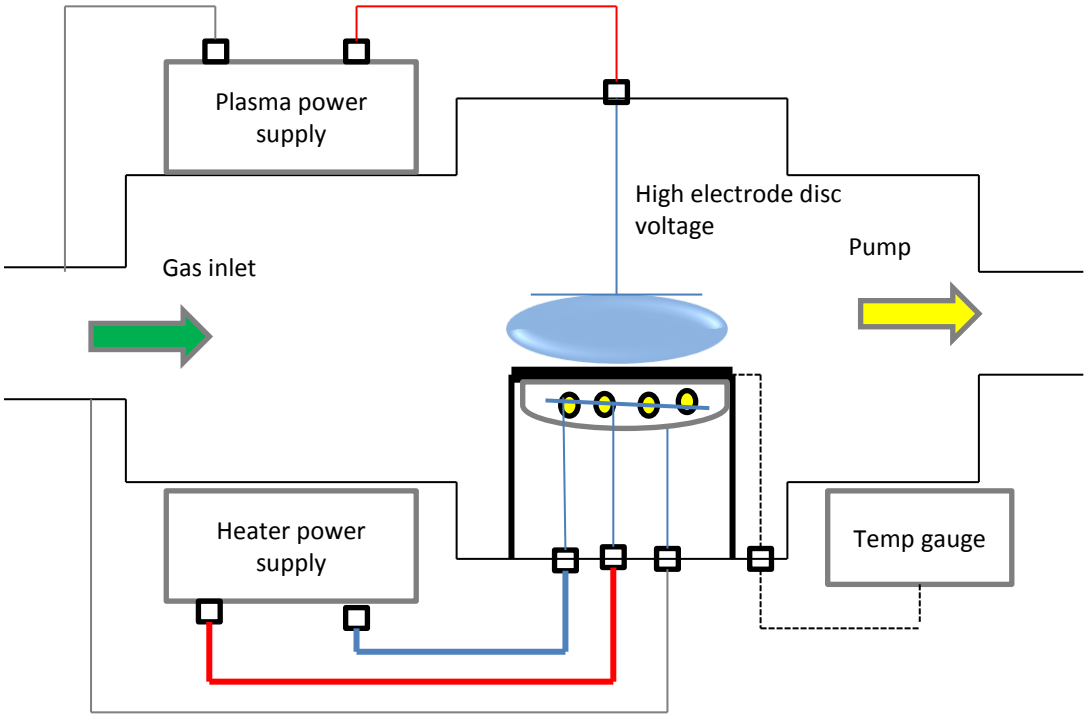

Figure 6: An illustration of plasma enhanced CVD reactor (Adapted from Hamedani et al., 2015)

2.3. Catalyst for CNTs/CNT yarn Production

In CCVD, substances that are able to decompose hydrocarbons and form CNTs are used as catalyst. Common catalysts used in CCVD are transition metals in the form of nanoparticles since they are good in promoting the CNT growth. There are three characteristics of transition metals that enables CNT growth and this are; the catalytic activity of decomposing volatile

carbon compounds, the ability of metastable carbide formation and the ability of carbon to diffuse through and over metal particles (Danafar et al., 2009).

CCVD process consist of three microscopic steps which are; the dissociation of hydrocarbons molecules by catalyst, the saturation of carbon atoms in the catalyst particles and formation of CNT by precipitation of carbon from catalyst

According to Baker et al, the catalytic growth mechanism governing CNT growth is based on the vapour-liquid-solid (VLS) where the vapour atoms are absorbed by the liquid catalytic particles to form metal carbon solid state solution. When the solid state solution of metal carbons becomes supersaturated this leads to the formation of carbon nanotube through the precipitation of carbon on the surfaces of the solid particle (Sengupta et al., n.d).

When using CCVD methods, the catalyst can be introduced into the reaction by various ways such as; vapour or sputter deposition on a thin metallic layer on the substrate, through the saturation of porous materials by metal, deposition of solutions containing catalysing metals, or introducing organometallic substances into the reactor (Sengupta et al., n.d).

The better understanding of catalyst activity will improved the controlled CNT growth because CNT growth depends on the distribution of the catalyst in the reaction (Makris et al., 2005).

2.3.1. Supported Catalysts

Substrate/supported catalysts are used in fixed bed where a solid catalyst is placed inside the reactor and the carbon precursor is introduced when the reactor reaches a desired temperature. The main disadvantage of this process is the limitations of the reaction between the gas and the solid. Temperature gradient also affects the efficiency of the process severely (Danafar et al., 2009). Thin metal films are preferred for the production of CNTs on flat and patterned substrates to achieve aligned CNTs (Makris et al., 2005). For substrate catalysts, it is important to control the size and space of the catalyst for production of long vertically aligned CNTs. This is because research shows that the catalyst size controls the CNT diameter and the number of walls (Chen et al., 2017). Refer to Figure 7 for the illustration of horizontal CVD set-up.

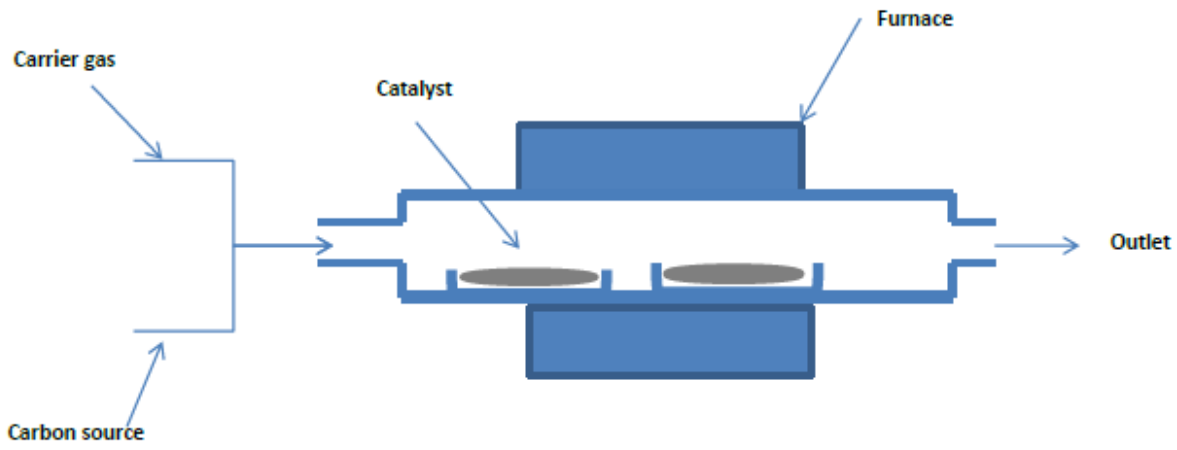

Figure 7: A reactor set-up for the supported/substrate catalyst (Adapted from Chen et al., 2017)

For supported catalyst, there are two growth mechanisms of CNTs known as root growth or tip growth. The root growth is when the catalyst stays attached to the surface during CNT growth. In tip growth, the catalyst migrates to the top of CNTs (Chen et al., 2017). Recent studies have indicated that the strength of the bond between catalyst and substrate dictate the type of the reaction mechanism. Root growth occurs when there are stronger interactions and tip growth is the resultant of weaker interactions of catalyst-substrate (Chen et al., 2017). The two mechanisms are illustrated in Figure 8 and Figure 9.

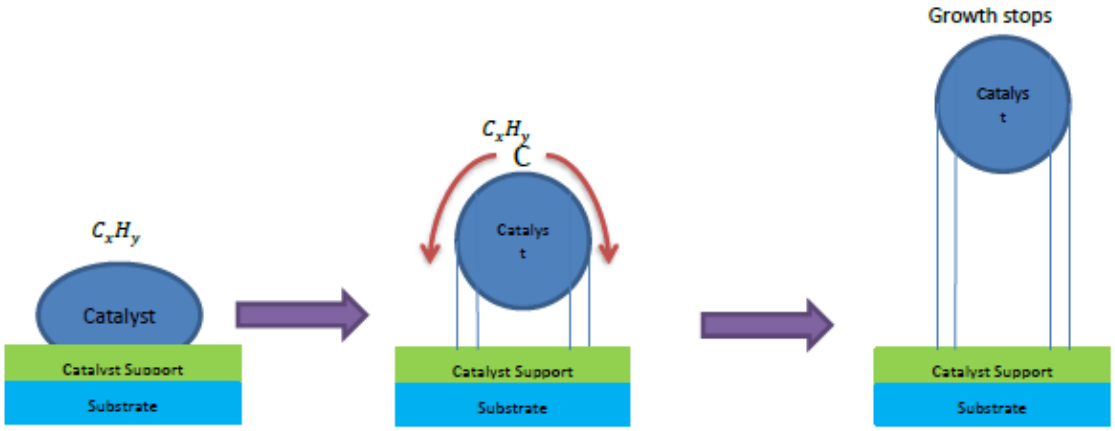

Figure 8: Tip growth mechanism (adapted from Chen et al., 2017)

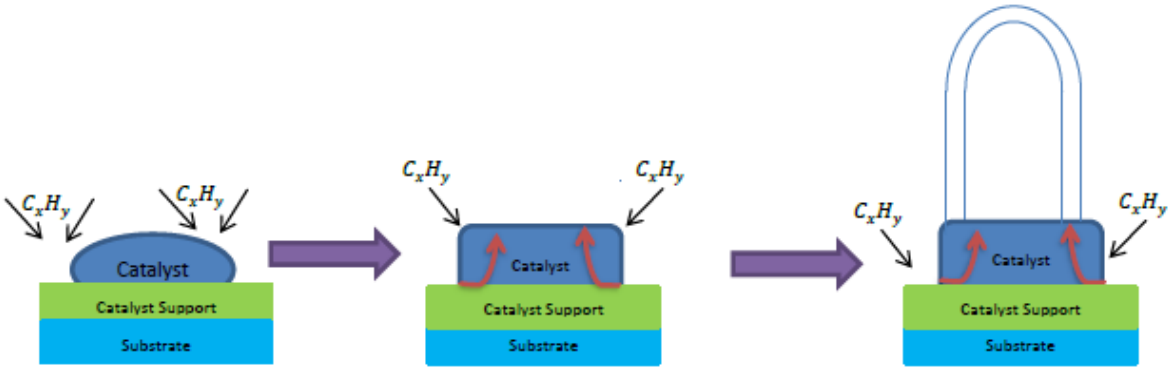

Figure 9: Root growth mechanism for CNT growth (adpted from Chen et al., 2017)

2.3.2. Floating Catalysts

In floating catalyst process a gas phase mixture of catalyst and reactants are carried into a reactor that is kept at high temperature where CCVD takes place. During the course of the reaction, the gas phase catalyst transforms into nano-sized solid phase active catalyst particles in situ. Metal transition powders are commonly used as floating catalyst for mass production of CNT bundles.

One of the challenges of using the floating catalyst is the difficulty in preventing the agglomeration of active catalyst particles. The catalyst particles that adhere to the reactor walls

increases their residence time of growing CNTs, whereas the unreacted gas phase catalyst and nano-catalyst left in the reactor are carried out by the unused reactants and carrier gases (Danafar et al., 2009). Figure 10 illustrates the set-up for CNT production using floating catalyst.

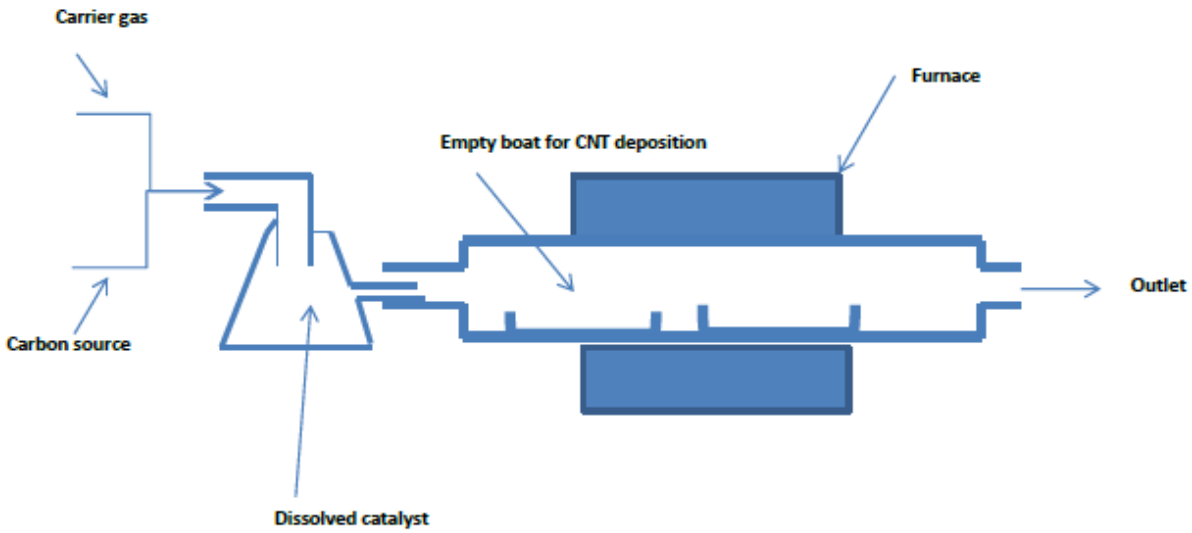

Figure 10: A reactor set-up for CNT production using floating catalyst

2.4.CNTs Purification

The production of CNTs often results in by-products such as amorphous carbon, fullerenes and metals used as catalyst during the reaction (Aqel et al., 2012). The existence of these impurities lowers the quality of the CNTs and aggressive treatments are often used to eliminate the impurities and enhance the quality of the CNTs. The use of purification processes is likely to affect the structure and yield of the produced CNTs (Hou et al., 2008).

Although purification methods remove the impurities on the CNTs, they however limit the analysis of CNT characteristics and affects CNT performance for new applications. However, most CNT applications rely on the purity of the CNTs hence it is vital depending on the CNT use to remove the impurities using various purification methods (Aqel et al., 2012). Purification methods that do not alter the structure of CNTs are preferred as this will enable researchers to fully utilize CNT properties (Hou et al., 2008). This section entails the chemical, physical and multi-step purification methods for CNTs (Ismail et al., 2008).

2.4.1.Physical Purification Methods

During physical separation, the synthesis products are separated as a function of size. Physical purification methods do not alter the morphology of the nanotubes, however it yields CNTs with low purity and involves complex procedures. Physical processes include; ultrasonication, filtration, centrifugation and size-exclusive chromatography.

2.4.1.1.Filtration

Filtration method employs the use of narrow size pore distribution membranes to eliminate impurities and to fractionate CNTs by length. The membranes are designed such that the CNTs are trapped by the filter while other impurities pass through the filter (Aqel et al., 2012). This method also separate according to aspect ratio and solubility of CNTs in specific solvents (Hou et al., 2008).

2.4.1.2.Ultrasonication

The use of ultrasound in the presence of solvents such as dichloromethane to remove impurities is referred to as ultrasonication. This procedure has been identified as the most effective method for removing amorphous carbon (Ismail et al., 2008). This method forces the agglomerates of nanoparticles to vibrate and become more dispersed. It is of great importance to carefully select the reagents because the separation of CNTs from impurities depends on the type of surfactant, reagents and solvent used. The duration of CNT exposure also matters because longer exposure time will cause the CNTs to react with the solvent (Aqel et al., 2012).

2.4.1.3. Chromatography

High Performance Liquid Chromatography (HPLC) or Size exclusion chromatography (SEC) can be used to purify CNTs and separate them according to their lengths (Ismail et al., 2008). This process is preferred for the separation of small quantities of CNTs into fractions with small lengths and diameters. The separation occurs in a column where CNTs are run in a porous material where they are allowed to flow. The most important factor is the pore size which controls the size distribution which can be separated (Aqel et al., 2012).

2.4.1.4.Chemical Purification Methods

Chemical purification processes separate all the produced substances as a function of reactivity. This method improves the purity of the CNTs except it compromises the CNT morphology and yield (Aqel et al., 2012). Controlled reaction conditions may prevent the altering of nanotubes

and the pentagonal structure at the ends of the tubes to preserve the CNT structure (Ismail et al., 2008).

Common types of chemical purification methods are; oxidation by heat, acid and oxidizing agents, alkali treatment and gas annealing (Mahalingam et al., 2012).

2.4.1.5.Oxidation

The preferred chemical method by far is the oxidation of CNTs in wet or dry conditions. Wet oxidation is when CNTs are oxidized in concentrated acids or strong oxidants and dry oxidation uses air or other gases to oxidize the CNTs at a controlled temperature (Mahalingam et al., 2012). Amorphous carbon and other carbon particles have a high oxidative activity thus this enables them to be reduced easily compared to CNTs (Ismail et al., 2008). This method is also favoured because metal catalyst acts as an oxidizing catalyst thus enabling the effective removal of impurities (Aqel et al., 2012).

2.4.1.6. Acid Treatment

Acid treatment is used to remove metal catalysts. For this process to take place, the metal catalyst will have to be exposed by sonication or oxidation (Mahalingam et al., 2012). The selection of acid is important because some acids have an effect only on metal catalysts while others have an effect even on the CNTs and carbon particles. For example, when using HNO_3 only metal catalysts will be eliminated whereas HCL will have some effect even on the CNTs. There are other factors such as reaction temperature, concentration, time and pressure that also affect the purification process and according to Aqel et al. these factors are not well understood yet (Aqel et al., 2012).

2.4.1.7. Annealing and thermal treatment

Annealing/thermal treatment uses high temperatures to remove impurities by rearranging CNTs (Hou et al., 2008). Other graphitic carbons pyrolyze at high temperatures while metal also melts when exposed to high temperatures thus favouring the separation process. The temperature range used for annealing is ranged between 873 -1873 K (Aqel et al., 2012).

2.4.1.8. Multi Step Purification Method

The removal of metal catalyst, amorphous carbon and other impurities can be done using both chemical and physical methods. This method is referred to as multi-step purification and is employed when a single treatment is not adequate to get rid of all the impurities. The use of

multi-step methods has been identified to be efficient as they yield CNTs with high purity and cause minimal damage to the tube walls (Ismail et al., 2008).

The table below summarizes the purification methods discussed above and their effect on CNT properties.

Table 1: A summary of purification methods and their effect on CNT Characteristics

Purification Methods		Description	References
Chemical Methods	Liquid oxidation	Remove catalyst, support and amorphous carbon. Tips open. Introduce functional groups	(Ovejero et al., 2006)
	Alkali treatment	Remove catalyst, support and amorphous carbon. Tips open.	(Jurmann et al., 2006)
	Microwave digestion	Remove catalyst, support and amorphous carbon. Reduced reaction temperature and acids used	(Hirsch et al., 2005)
	Gas phase oxidation	Remove catalyst, support and amorphous carbon. Tips open. Less damage to CNT structure	(Hiura et al., 1995)
	Halogenation	Facilitate the oxidation of reactive areas of CNTs	(Hirsch et al., 2005)
Physical Methods	Filtration	CNTs are separated according to length and diameter	(Zhang et al., 2014)
	Sonication	Enables solubility of CNTs in solvents. Introduce functional groups	(Yan et al., 2012)
	Chromatography	CNTs are separated according to length	(Speltini et al., 2010)

2.5.CNT Yarn Spinning Methods

There are liquid and solid methods of converting individual CNTs into CNT yarns. Liquid method is where the CNTs are dispersed into the liquid and solution then spun into fibers (Liu et al., 2010). Solid methods CNTs are directly spun into ropes or yarns. However this method produce yarns with properties which are not close to optimal. When producing CNT yarns, the length, chirality and process ability affect the properties of the yarn. When producing CNT yarn, it is aimed at producing close properties of individual CNTs (Behabtu et al., 2008).

The types of spinning methods used have an effect in the electrical conductivity of the yarn. Wet methods have shown to result in poor conductivity as compared to the direct dry spinning method (Lekawa-Raus et al., 2014).

Liquid state method has challenges because of difficulties in processing nanotubes in the liquid phase. This is because CNTs are not soluble in aqueous or organic solvents and they do not melt because of their high stiffness and they have higher molecular weight (Behabtu et al., 2008). Moreover, this method results in impurities in CNTs due to surfactants or polymer molecules (Liu et al., 2010). It is easy for CNTs to form bundles due to the strong Van der Waals forces between their walls and this is not good because nanotubes cannot be controlled and aligned when in a solution unless if they are dispersed in SWCNTs. One of the ways of making CNTs more soluble is to functionalize CNTs with side groups that make them soluble in common solvents. This method is not viable because it destroys the electronic properties of CNTs (Behabtu et al., 2008).

Wet and dry spinning methods of CNT into CNT yarns have been practiced, however the yield produced is very small (Wang et al., 2013). These methods are briefly explained below.

2.5.1. Forest Spinning

This method converts CNT bundles into yarn by aligning and stretching the bundles during spinning (Tran et al., 2011). Liu et al reported a twisting and shrinking method. In this method, CNT array were twisted and then passed through a volatile solution for shrinking. Various shrinking solutions were used such as ethanol, water and acetone, where acetone resulted in best yarn with high strength of 1 GP (Ghemes et al., 2012). Jayasinghe et al obtained good yarn with high mechanical strength and high electrical conductivity by spinning from two aligned CNT arrays where heating and tensioning were applied during spinning (Jayasinghe et al., 2013). Ghemes et al. (2012) achieved a yarn with strength around hundred MP through high speed drawing and twisting.

2.5.2. Direct Spinning

Direct spinning method spin CNTs into CNT yarn directly from the furnace using a floating catalyst. It allows continuous production of a yarn with good properties. More impurities are experienced in the yarn from the catalyst depositions when using direct spinning method

(Jayasinghe et al., 2013). The following figure illustrates direct spinning of CNTs into CNTs done by researchers in the past.

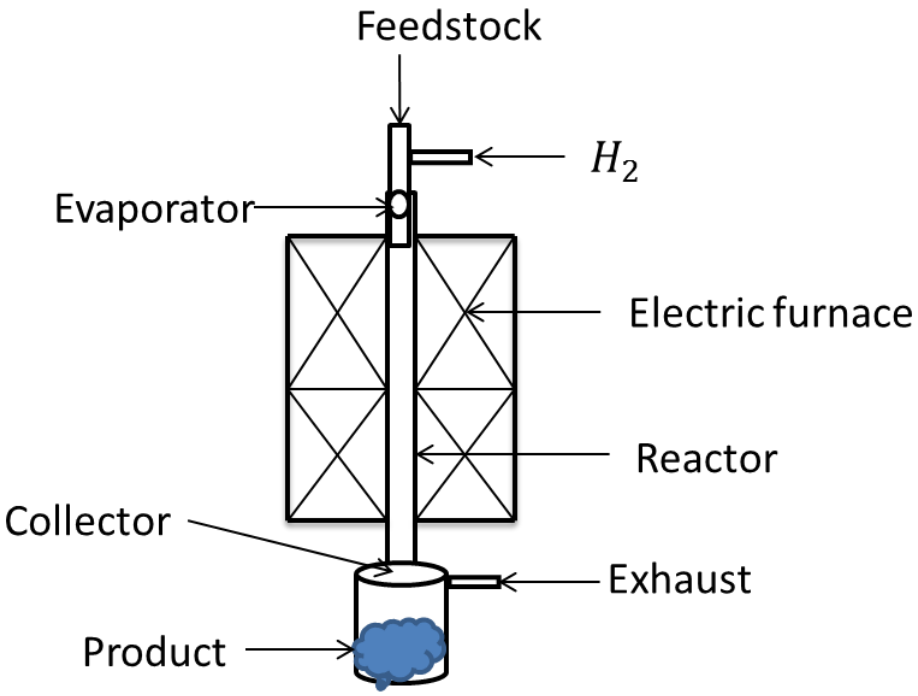

Figure 11: An illustration of direct spinning method of CNTs (adapted from Choo et al., 2012)

2.5.3.Surfactant Based Coagulation

This method stabilizes CNTs by preventing them from bundling together again (Behabtu et al., 2008). This is done by dispersing CNTs in the aqueous solution that contains surfactants and the solution is then sonicated therefore breaking CNTs bundles (Jayasinghe et al., 2013). Concentration of the surfactant plays a very important role in the stabilization of CNTs because if it is low CNTs will not be stabilized adequately. If the surfactant concentration is too high then depletion-induced aggregation will occur. Common surfactants that have been used include; Sodium Dodecyl Sulfate (SDS), Tetra-trimethylammonium bromide (TMB) and Lithium Dodecyl Sulfate (LDS). Here coagulants are used to aid the SWCNTs to form fibers by flocculation. Various methods can be used to improve the SWCNTs content in the fiber to improve mechanical and electrical properties. One way is to spin the yarn in the PVA solvent and the dry as this increases Young's Modulus and tensile strength of the yarn (Behabtu et al., 2008).

There are various factors that affect surfactant spinning; however the most important factor is the concentration of the surfactant for adequate stabilization to occur. The surfactant stabilized is then coagulated in a rotating coagulation bath and coagulation solution is pumped out. PVA is the common coagulant that is used (Behabtu et al., 2008).

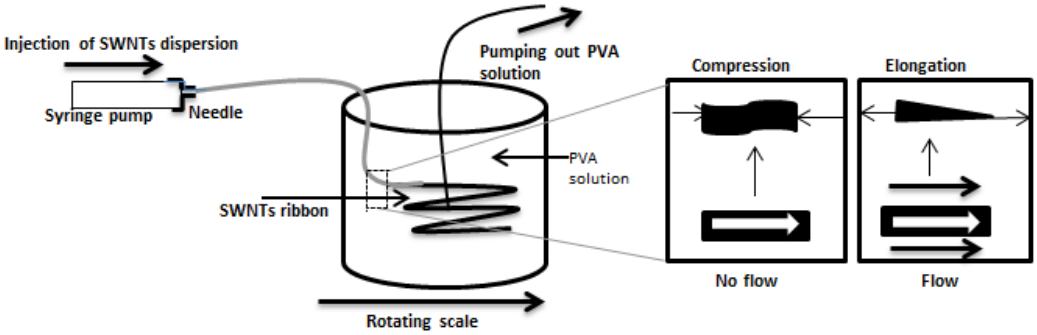

Figure 12: A setup for coagulation spinning of CNTs (adapted from Behabtu et al., 2008)

2.5.4. Liquid-crystalline Spinning

Super acids are used as solvents to dissolve CNTs to form liquid-crystalline phase. CNTs; specifically single-wall carbon nanotubes (SWCNTs) behave like rigid rods when dissolved in super acids. High acid concentration results in fully liquid-crystalline solution. The fibres formed when using liquid crystallization spinning method are highly aligned even before post-treatment (Behabtu et al., 2008).

Lower concentration causes SWCNTs to be randomly orientated in the solution, intermediate concentrations results in the formation of biphasic equilibrium between coexisting isotropic and liquid-crystalline phase. The latter is explained depicted by Figure 5 below. Factors which affect specific boundary phases are SWCNTs length, polydispersity and solvent quality. Liquid-crystalline dopes containing high concentrations of SWCNTs yarns can be achieved when using super-acids. Acid-spun process results in best CNT fiber with good electrical conductivity but low mechanical properties. It is used in shorter SWCNTs and not in MWCNTs an longer SWCNTs. Researchers believe that if acid spinning can be adapted for shorter SWCNTs, then neat scalable fibers can be produced (Behabtu et al., 2008).

Figure 13 illustrates the effect of acid concentration on the CNT yarn formation by using liquid crystallization method.

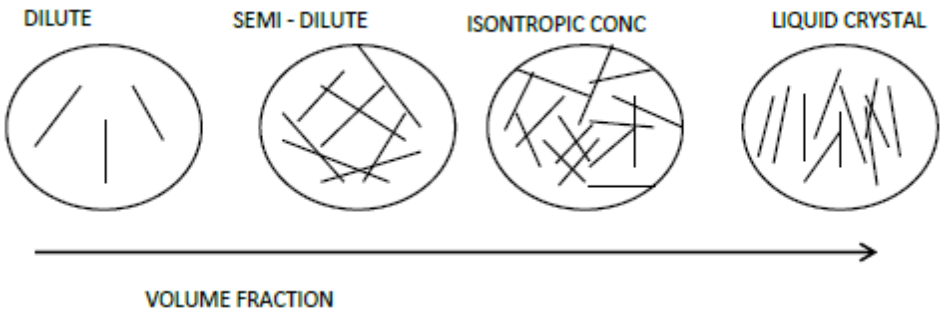

Figure 13: The effect of acid concentration on the CNT yarn formation (adapted from Behabtu et al., 2008)

2.6. Characterization Techniques

The excellent properties of nanotubes have increased the interest of studies in nanotechnology. To fully understand the properties of nanotubes, various characterizing methods are used to characterize size, crystal structure, elemental composition and other physical properties. More than one technique can be used to evaluate the same physical property which increases the chance of acquiring precise results (Mourdikoudis et al., 2018). It is however, important to understand the advantages and disadvantages of each technique in order to best select the necessary technique for assessing nanotube properties.

2.6.1. Thermal Gravimetric Analysis (TGA)

The method of thermal gravimetric analysis (TGA) is used to estimate the purity of CNT and the concentration of impurities attached to the CNT sidewalls. This process measures the decline in sample mass as a function of change in temperature. TGA gives a quantitative data of the weight fractions of carbon and metal catalysts in the sample (Aqel et al., 2012). An estimate of metal catalyst can also be given from the residuals after all organics have been volatilized. To obtain high quality of TGA data large amounts of CNTs are required because this technique depends on the quantity of CNTs used (Wepasnick et al., 2009).

One of the challenges in TGA is the difficulty in interpreting the data due to close proximity of various peaks (Wepasnick et al., 2009).

2.6.2. Electron Microscopy

Electron microscopy is an essential tool used to evaluate the size, shape and structure of nanomaterials. This process is defined as an imaging technique that uses electron beam to probe the material. The electron beam with uniform current density is exposed on a thin sample to image the specimen. There are two types of electron microscopy namely; scanning electron microscopy (SEM) and transmission electron microscopy (TEM). Both SEM and TEM are used to evaluate the morphology and purity of nanomaterials (Medjo, 2013). SEM and TEM methods yield the characterization data on the surface features of the sample, specimen size and shape, the elements and compounds making up the samples (Aqel et al., 2012).

TEM employs the use of high energy beam to image samples based on electron transmission (Wepasnick et al., 2009). TEM can be used in low and high magnifications for different evaluations. In low magnifications TEM measures the length and dispersion state of CNTs (Aqel, et al. 2012). At high magnifications the following can achieved; to count the number of walls in MWCNTs, measurement of inner and outer diameters, to identify the structural changes and asses the structural integrity (Wepasnick et al., 2009).

The limitation of SEM and TEM is the damages to the sample material from using the electron beam. Moreover, the sample needs to be in vacuum (Medjo, 2013). To mitigate the CNT sidewall damage, it is recommended to expose the sample to shorter durations of less than 15 seconds and use beam energies of not more than 100 KeV (Wepasnick et al., 2009).

2.6.3. Raman Spectroscopy

Raman spectroscopy is used to identify the types of CNTs in the characterized sample. During the characterization, the sample is exposed to intense laser light that produces energy scattered photons which are used to identify vibrational modes (Wepasnick et al., 2009). This procedure uses G-band and D-band to analyse the specimen. The G-band is a property of graphitic layer and resembles the tangential vibrations of carbon atoms. The D-band is a measure of defective graphitic structures (Costa, 2008). Raman spectroscopy measures the quality of the bulk sample by comparing the intensity ratios of the G-band and D-band (Wepasnick et al., 2009). In addition to the two characteristic modes, there is a third mode that is sensitive to the diameter of the SWCNT namely radial breathing mode (RBM) (Aqel et al., 2012).

The information provided by Raman spectroscopy includes the vibrational properties and electronic structures of CNTs which gives more insight to the diameter and purity of the samples studied (Costa, 2008).

There are four types of the features that are sensitive to the chiral indices (n,m) and these are; the RBM, the D-band, G-band and the harmonic G'band (second order of G-band). G' band is observable in carbons that do not have defects. The G-band characteristic depends on whether the nanotube is semiconducting or metallic. The comparison of the D-band, G-band and RBM allows the identification of the type of CNTs present in the sample (Costa, 2008). According to Aqel et al. (2012) the frequency of RBM is less than 200 cm^{-1}, D-band having frequency around 1340 cm^{-1} and lastly G-band with the frequency between 1500 – 16000 cm^{-1}. The limitation of Raman spectroscopy is the inability to provide the quantitative information of the type of CNTs in the analysed sample (Costa, 2008).

2.6.4. Four-Point Probe

Four probe method is used to evaluate the electrical properties of solids and thin films. This technique is favoured due to its simplicity in sample preparation and high accuracy. There are various measurement theories used for the four probe such as van der Pauw mode, collinear mode, square mode and dual probe configuration mode. Collinear mode is the most common mode employed by researchers. In collinear mode, current is passed through the outer probe pair while voltage drop is measured across the inner probe pair. Figure 14 illustrates the four probe setup.

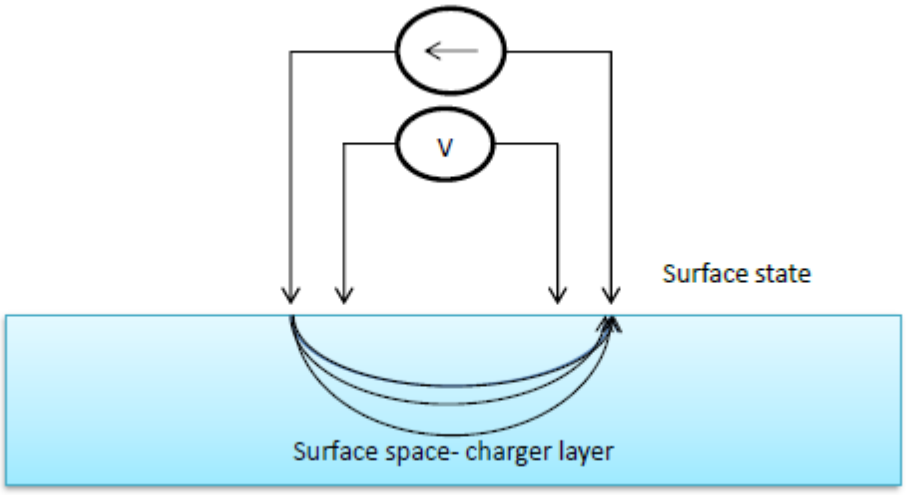

Figure 14: A common set-up for four probe method

2.7. Parametric effect of production variables and optimization

2.7.1. Effect of production variables and methods of investigation

From the investigation methods explained in Section 2.2, arc discharge and CVD methods are the most utilized processes for CNT synthesis. This section contains the effect of process parameters when using arc discharge and CVD methods.

2.7.1.1. Effect of production variables in arc discharge

During CNT production when using arc discharge, it is necessary to use a catalyst if SWCNTs are desired. This is because in the absence of a catalyst the only products that formed are the soot and deposit which contains fullerenes, MWCNTs and graphite carbon nanoparticles. The evaporation of the metal catalyst with carbon in arc discharge produces SWCNTs in addition to the MWCNTs and graphite carbon nanoparticles. The nucleation and growth of CNTs in arc discharge are mainly affected by the carbon vapour concentration, carbon vapour dispersion in inert gas, the reactor temperature, catalyst composition, the presence of hydrogen and the addition of promoters. The above mentioned factors also affect the CNT diameters and the type of CNTs that is formed (Szabo et al., 2010).

With arc discharge method, the CNT yield decreases when pure hydrogen is introduced during the reaction. It has been proven that the use of Nickel (*Ni*) as a catalyst in arc discharge method produces only collar-like assemblies of SWCNTs and SWCNTs ribbons (Szabo et al., 2010).

The use of sulphur containing catalysts or the addition of sulphur in the arc discharge rector produces Doubled walled carbon nanotubes (DWCNTs). This is due to the ability of sulphur to enhance the formation of filled CNTs. Hydrocarbons from the benzene group such as Toluene improves the purity of the CNTs when used as carbon precursors (Szabo et al., 2010).

The use of aqueous solutions such as liquid N_2 and deionized water and the voltage used have an effect on the type of CNTs produced. For example; the use of liquid N_2 at higher voltages produced SWCNTs while MWCNTs and amorphous carbon were produced at lower temperatures (Szabo et al., 2010). The pressure of carrier and inert gases also affect the type of CNTs produced. For example; SWCNTs were achieved when the high pressure of Helium (He) was used and whereas a mixture of fullerenes was obtained at lower pressure in arc discharge (Szabo et al., 2010).

2.7.1.2. Effect of production variables in CVD

CVD method is the main technique that allows for the selective production of CNTs with excellent properties. The horizontal configuration of CVD reactor is used with supported catalysts for CNT synthesis while the vertical CVD reactor is mostly employed for floating catalysts often used for mass production (Khavarian et al., 2013).

The most important parameters in CVD method is the reactor temperature, the operating pressure, the size of the catalyst, hydrocarbon volume and concentration, the nature of catalyst support and the reaction duration. CNT length depends mostly on the time it takes to complete the reaction.

Transition metals are used as catalyst for the synthesis of SWCNTs and MWCNTs when using CVD method. Furthermore, researchers have reported that rare earth oxides enhance the activity and selectivity during CNT formation as co-catalysts. The growth and morphology of CNT heavily depends on the catalyst selection. Iron (Fe), cobalt (Co) and Nickel (Ni) are the most commonly utilized metal catalyst in CVD method. Fe containing catalysts promotes the growth of SWCNTs (Szabo et al., 2010).

Gas phase catalysts/floating catalysts are favoured in the continuous production of CNTs due to the reason that CNTs are free from the catalyst support. A continuous process is easy to carry out when using gas phase catalysts. Supported catalysts are desired for in-situ synthesis of CNTs and the substrate and catalyst dictate the structure of the tubes. The size of the catalyst affects the diameter and type of CNTs formed (Szabo et al., 2010).

2.7.2. Investigation of parametric effect using response surface methodology (RSM)

RSM is one of the DOE techniques used to model experimental responses. RSM is used to minimize the number of runs one should carry out during experimentation to save time and effort. RSM is also used to predict accurate mathematical models (Bratz, 2016) Many researchers have considered RSM as more efficient and a simple optimization technique.

RSM in this study was used to analyse the effect of various operating parameters and their interactions on the CNT/CNT yarn yield purity and electrical conductivity (Bratz 2016).The main functions of RSM are to analyse various process conditions, to design experiment, to reduce the number of experiments, to evaluate the effect of process variables and to find the optimal parameters to yield desirable process yield (Aydar, 2018). RSM has two main experimented designs and these are the Box-Behnken design (BBD) and Central composite design (CCD). BBD is often used to decrease the number of experiments that achieve quadratic interactions between selected factor pairs (Rajamani et al., 2018).

The Objective of using RSM is to optimize the response. The parameters that affect the process are called independent variables whereas responses are dependent variables. In RSM, the experimental data are aligned to either of the following statistical models, linear quadratic, cubic or two factorial interactional (2FI). Three factors namely correlation of coefficient (R^2), adjusted determination coeff (Adj-R^2) and adequate precision are used to check model accuracy. The model is considered adequate when the P value < 0.05, lack of fit P value >0.05, R^2>0.9 (Aydar, 2018).

2.7.2.1. Optimization study via RSM

The optimization using RSM followed the steps highlighted in Figure 15 (adapted from Lenth, 2012).

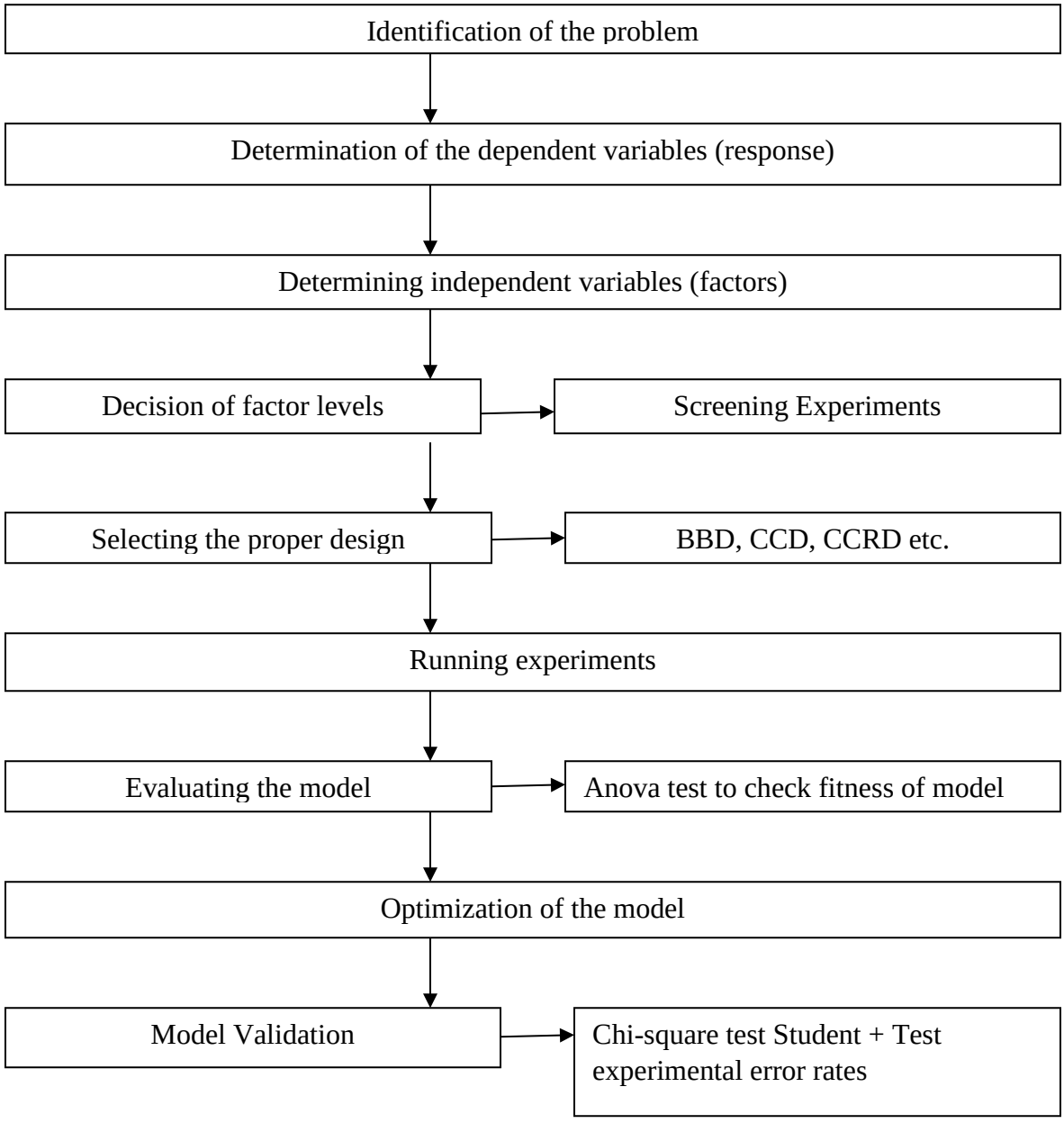

Figure 15: Steps used to optimize the respond using RSM methodology

CHAPTER THREE

3.0. Methodology

3.1. Synthesis of CNTs and CNT yarn using CCVD reactor

For a better understanding of the effect of process parameters on optimization of CNT yarn, an experimental study was performed where the reaction temperature, carbon precursor flowrate and the catalyst state were varied. CNTs were produced in a swirled continuous CVD reactor using methane as carbon source and ferrocene as a catalyst to investigate the effect of reaction temperature, methane flowrate and catalyst state on the yield and quality of produced CNTs. Ferrocene was used in solid and liquid states where in liquid phase it was dissolved in cyclopentane. Three important stages that were undertaken during the course of research are summarized in Figure 16.

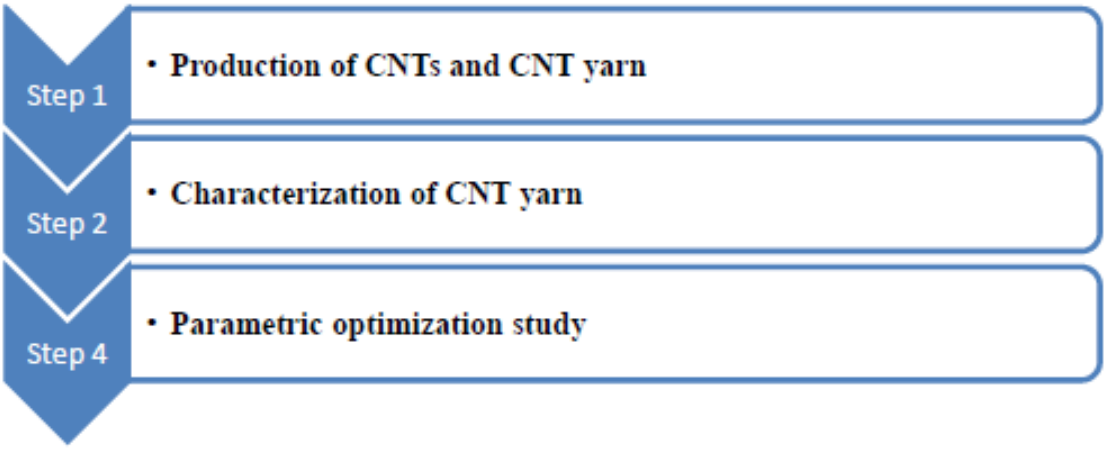

Figure 16: Stages undertaken during the research study

3.1.1. CNTs synthesis

During the production, 10 g of Ferrocene ($F_e(CO)_5$) catalyst was vaporized at 300^{o}C in the vapourizer attached to the reactor and the vapourized catalyst was carried to the reaction zone, where methane and hydrogen gas were introduced, by argon gas. The flow rate of methane, argon and the hydrogen gases into the reactor were 150 ml/min, 150 ml/min and 50 ml/min, respectively. The reaction zone (inside the CVD reactor) was maintained at reaction temperature of 850^{o}C and the reaction was run for 15 minutes. The temperature at the reaction zone was measured with a PT100 thermocouple and controlled with PID controller built with the reactor. To gain insight into the effect of temperature on the yield and quality of produced CNTs, the reaction temperature was varied from 900^{o}C to 1000^{o}C at a step change of 50^{o}C.

To investigate the effect of changing the state of catalyst from solid state to liquid state on the quality and yield of CNTs produced in the reactor, 10 g of Ferrocene powder was dissolved in 10 ml of cyclopentane. The liquid solution was vaporized at 300^{o}C in the vapourizer attached to the reactor and the vapourized catalyst was carried to the reaction zone, where methane and hydrogen gases were introduced, by argon gas. The flow rate of the carbon source, argon and hydrogen gases into the reactor were 150 ml/min, 150 ml/min and 50 ml/min, respectively. The reaction zone (inside the CVD reactor) was maintained at reaction temperature of 850^{o}C and the reaction was run for 15 minutes. The same experiment was repeated while varying temperature from 900^{o}C to 1000^{o}C. Figure 17 depicts the experimental setup using to manufacture CNTs.

Figure 17: An experimental setup for CNT production

3.1.2.CNT yarn synthesis

Similarly with CNT production, a swirled CCVD reactor was connected to a spinning motor to produce CNT yarn when the flow of methane, hydrogen and argon gas were present in the reactor at various temperatures. Direct spinning method from the reactor was used to convert the produced CNTs into CNT yarn. Through changing the catalyst state in section 3.2 it was realized that the quality and yield of CNTs were better when Ferrocene was dissolved in cyclopentane thus a solid Ferrocene was not used in producing CNT yarns. The reaction temperature was varied from 850℃ to 1000℃ at a step change of 50℃. Furthermore, methane flow rate was varied between 150ml/min and 160ml/min.

3.2. Characterization of CNTs and CNT yarn

3.2.1. Scanning electron microscopy

Carl Zeiss Sigma FESEM equipped with oxford x-act EDX detector was used for imaging samples. Firstly the samples were placed on the carbon tape that was on the stub. Then all CNTs and CNT yarn samples were sputter coated using Pd-Au nanometer coating. The samples were

then placed onto the SEM chamber which was then pumped to high vacuum. The in-lens and secondary detectors were used to analyse the samples. EDX detector was used to obtain the elemental composition of the samples. During imaging, the voltage of 10 keV was used.

3.2.2. Raman Spectroscopy

The characterization of both CNTs and CNT yarn sample for purity, Raman Spectroscopy was used. The first sample was tested at with laser 514.5 nm using 0.40 mW. The spectra were slightly noisy due to low incident power thus the laser power was adjusted to 40 μW with the same laser line of 514.5 nm.

3.2.3. Four-point probe

Four-probe point equipment was used to measure the current and resistance of the synthesized CNTs and CNT yarns. Firstly the samples were placed on the double sided tape which was placed on the non-conducting glass. The prepared samples were then analysed under the four probe point microscope that obtained the contact resistance at the CNT terminal interface. The calculations were then developed to obtain the CNT current.

3.3. Optimization via RSM approach

The Response Surface Methodology (RSM) was used to optimize the results for this study. The process optimization was performed for CNT yarns using the two most important responses designated by the letter "Y" where Y1 indicates yield (mg) and Y2 indicates the electrical conductivity.

The experiment chose two process factors to study for the CNT yarn production and optimization. These factors are indicated in the table below with their names used in the optimization study.

Table 2: Factors for RSM study of CNT yarns

Factor	Units	Range
A: Temperature	℃	900 – 1000
B: Methane flow rate	mg	150 – 160

The experiment was designed with Design – Expert 12 software using the Central Composite Design (CCD) from RSM techniques. A 2-level factorial option was selected and numerical factors were inserted including their levels from low to high. The full type option was used for CCD and response names and units were entered.

After completing the above, the design layout with 7 runs was created. Based on the design layout, scatter plot was created using factors varied in the RSM experiment. The results were analysed to determine whether they fit linear, two-factor interaction (2FI), quadratic and cubic polynomials. The best fit was selected based on the fit summary. The ANOVA was used to analyse the variance for the chosen model. Coded equation based on the selected model was created and the model was diagnosed based on its statistical properties. The model graphs such as contour plot and 3D surface plots were then created.

CHAPTER FOUR

4.0. Production of CNTs, CNT yarn and effect of state of catalyst

4.1. Introduction

Carbon nanotubes (CNTs) were first discovered in 1991 by Ilijima (Rafique et al., 2011). Most emerging engineering industries are made possible by the discovery of CNTs such as lightweight and heavy-duty industrial applications (Yaosef et al., 2016).

However, CNT bundles have shown poor properties as compared to individual CNTs. This is due to the low bulk density and a broad size distribution that is below $100\mu m$ (Wang et al., 2002). There are various methods of producing CNTs and these include; arc discharge, chemical vapor deposition (CVD), laser ablation, flame synthesis etc. CVD method is preferred for large scale production of CNTs because it is simple, easy to control the process and energy efficient (Rafique et al., 2011). This study employs CVD method since the aim is to produce high yield CNTs with good quality.

The use of macroscale nanotubes has proved to be more effective than using microscale CNTs, thus for this research it was important to spin the synthesized CNTs. However, research proves that the properties of CNT nanostructures such as yarns and sheets are still significantly lower compared to those of individual CNTs (De Volder, Tawfick, Baughman, & Hart, 2013). De Volder reports that CNT yarn produced from high-quality few-walled CNTs obtained stiffness of $357\ GPa$ and a strength of $88\ GPa$ having $1mm$ CNT gauge length. CNT yarn is still however an excellent conductor when compared to other materials such as copper, silver and aluminum. The table below compares the properties of CNT yarn with that of other good conductors (De Volder et al., 2013).

Table 3: A comparison of CNT yarn properties with some good conductor

Properties	Silver (Ag)	Copper (Cu)	Aluminium (Al)	CNT
Conductivity (MS/m)	63	59.6	35	100
Resistivity (1/K)	0.0038	0.00386	0.0039	˜Slightly positive
Density (kg/m^3)	10900	8960	2700	1500

CNT yarn properties are poor compared to those of individual CNTs because CNT yarn is made up of short CNTs therefore reducing the van der Waals forces between individual CNTs (Jayasinghe et al., 2013).

There are post treatment methods used to enhance the quality of CNT yarn such as polymer dip coating. This method only improves the mechanical properties of CNT yarn and results in decreased electrical conductivity (Choo et al., 2012). High temperature annealing is used to improve the electrical and thermal conductivities of CNT yarn. This method is not favoured due to the high costs associated with it. Moreover, CNT yarn treated by high temperature annealing becomes brittle (Jayasinghe et al., 2013).

4.2. Experimental procedure

CNTs were produced using a vertical CVD reactor and methane as carbon source. Ferrocene was used as a catalyst. To clearly investigate the effect of catalyst state; ferrocene was dissolved in liquid hydrocarbon (cyclopentane) and CNTs were produced using solid state catalyst only and liquid state catalyst. Argon was introduced in the system for 10 mins for flushing creating inert environment and also for checking for leaks. Catalyst of $7\ g$ was placed into the vaporizer and heated at $300℃$. The desired temperature of the furnace was varied between $850℃ - 1000℃$ using step change of $50℃$. The flow rates of the gases (Ar_2, H_2, CH_4)were introduced into the system at $150\ ml, 50\ ml$ and $150\ ml$ respectively. Ferrocene was allowed to be carried by the gases into the reactor for about 15 minutes. After the reaction, all the gases were stopped except for argon which was used to cool the system for 10 minutes. Then the reactor was left to cool for about 30 minutes and thereafter collecting samples.

The morphology and elemental composition of the CNTs were verified using scanning electron microscopy (SEM). Raman spectroscopy was used to analyze the degree of defect and graphitic formations. The electrical conductivity of the CNTs was analyzed using four-point probe method.

4.3. Results and discussion for CNTs

4.3.1.SEM images produced at reactor temperatures between $900 - 1000\ ^{0}C$

It is evident from Figure 18 to Figure 19 that when catalyst state is changed to liquid by dissolving ferrocene in cyclopentane; the morpholgy of the CNTs gets improved. From Figure 20 (b) the CNTs produced with liquid state catalyst are more pronounced and free of impurities compared to the CNTs in Figure 20 (a). At temperature of 950℃, CNTs produced with liquid catalyst are more aligned and longer than CNTs than CNTs formed from solid ferrocene. This could be due to the reason that research showed that straight, single-walled CNT are more likely to form at higher temperature whereas multi-walled CNTs form at lower temperatures (Sharma et al., 2007). The best CNTs achieved in terms of morphology and purity were obtained at the temperature of 950℃.

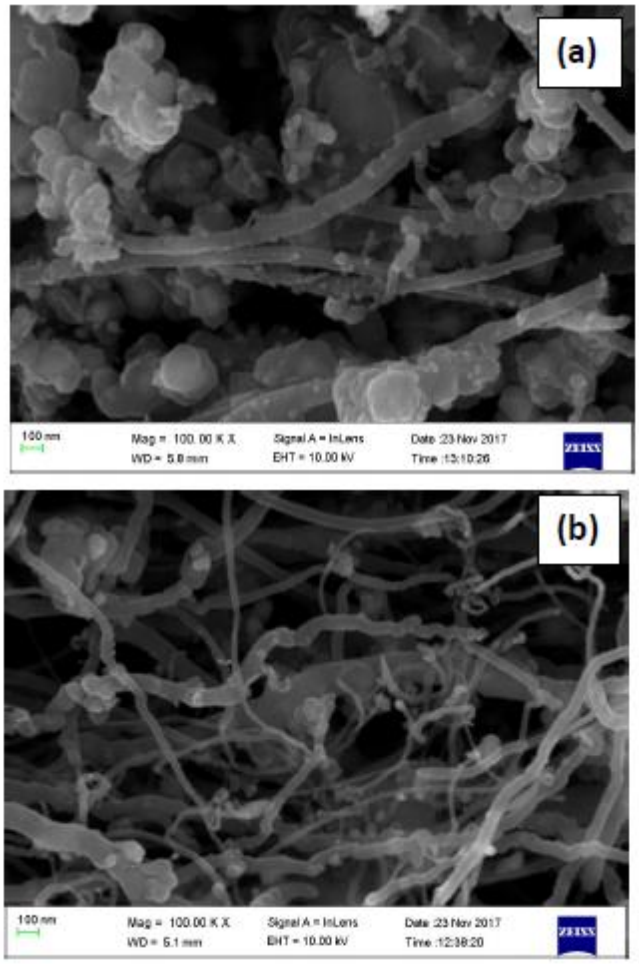

Figure 18: SEM produced at 900 ℃ (a) Solid ferrocene used (b) Ferrocene dissolved in cyclopentane

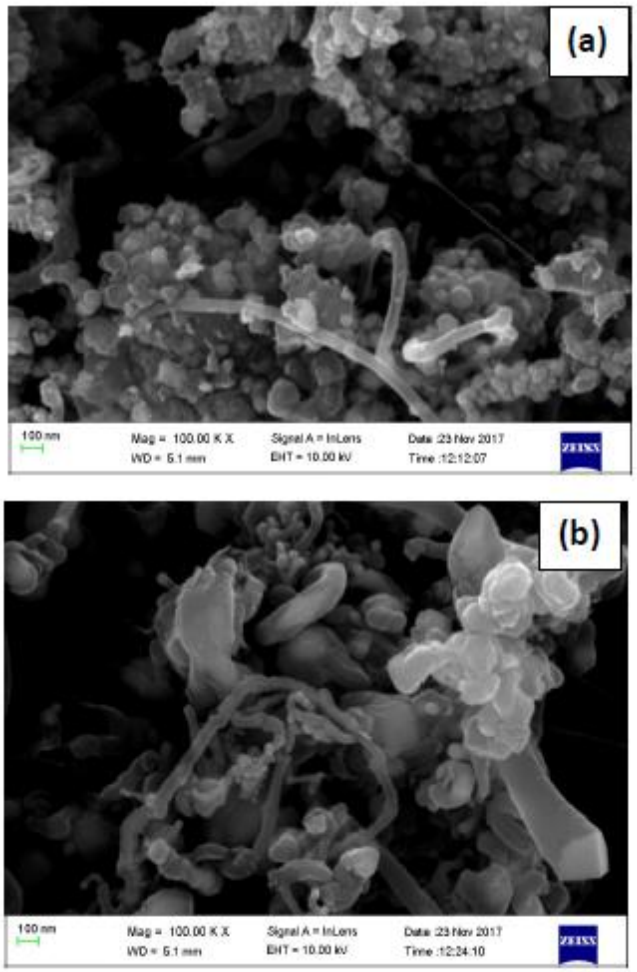

Figure 19: SEM produced at 950 ℃ (a) Solid ferrocene used (b) Ferrocene dissolved in cyclopentane

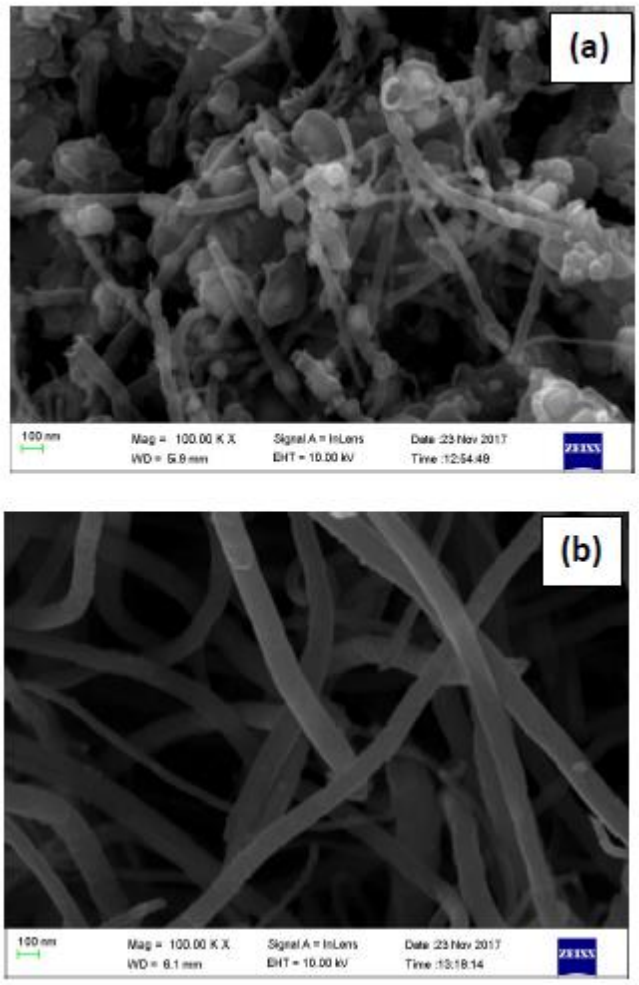

Figure 20: SEM produced at **1000** ℃ (a) Solid ferrocene used (b) Ferrocene dissolved in cyclopentane

4.3.2.Effect of temperature and catalyst state on CNT yield of CNTs

It is evident from the graphs in Figure 21 that CNT yield is higher when cyclopentane is used to dissolve Ferrocene. The reason of obtaining higher yield when using liquid catalyst could be the fact carbons in the cyclopentane also take part in the reaction therefore adding to the existing carbons in methane and Ferrocene which then increases the concentration and availability of active carbons thus increasing the CNT yield. The increasing CNT yield for both graphs from 850 ℃ to 900ºC conform with Aksak et al. (2009) research where increasing reaction temperature from 850ºC to 925ºC increased the length of CNT bundles. The drop in yield after

900ºC could be due to the effect of formation of amorphous carbon which then decreases the total formation of CNT bundles (Awasthi et al., 2005).

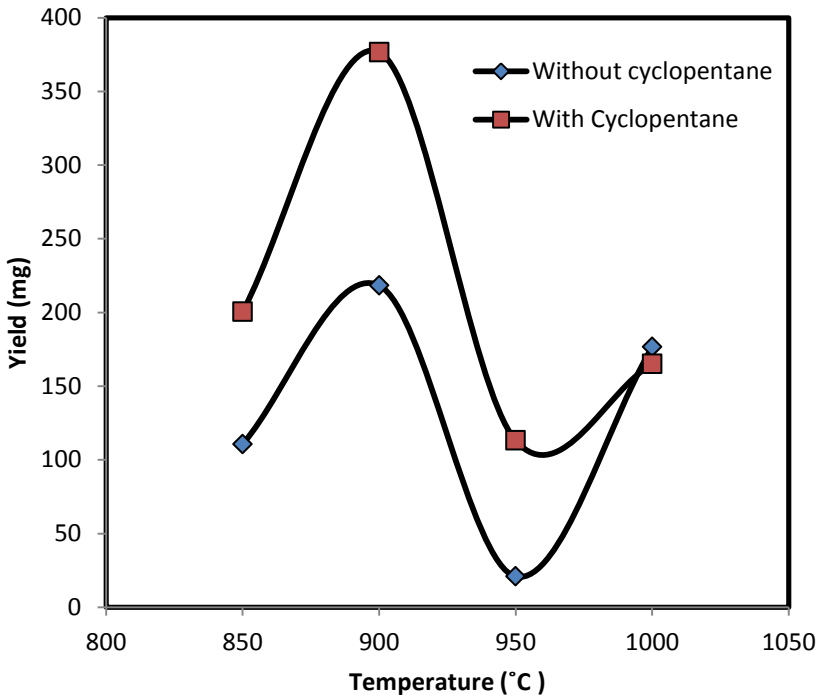

Figure 21: Effect of temperature and catalyst on CNT yield

4.3.3. Raman Spectroscopy Results

This subsection consists of the results from Raman Spectroscopy that showcase the purity of the samples produced. Here only CNT samples are analysed. For all the samples; a lower power setting of 40 μW was used.

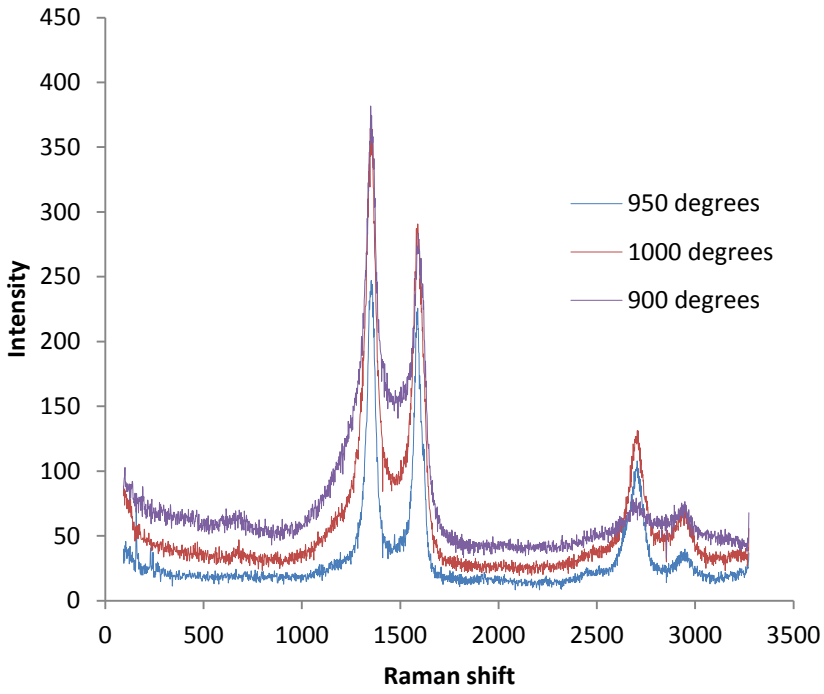

Figure 22: Raman results for CNTs produced at various temperature

The following table summarizes the I_D/I_G ratios of CNT production while reactor temperature and catalyst state were varied.

Table 4: I_D/I_G ratios of CNT production

Reaction temperature (℃)	**I_D/I_G**	**Catalyst state**
900	0.59	Solid
950	0.47	Solid
1000	0.34	Solid
900	0.57	Liquid
950	0.38	Liquid
1000	0.16	Liquid

The Raman results from the table above decreases with increasing temperatures. This means the purity of the synthesized CNTs improves at higher temperatures, again this observation could be due to an increase in the number of Sp^2 bonds in the reaction at high temperatures (Igbokwe et al., 2019). Moreover the CNTs manufactured using liquid Ferrocene have I_D/I_G ratio that is closest to zero. This observation indicates that the purity of CNTs produced with the dissolved ferrocene is high. The closer the I_D/I_G intensity ratios get to zero, the lesser the impurities are found in the CNTs (Awasthi et al., 2005).

4.3.4. Analysis by four-point probe

The electrical conductivity results for CNTs are illustrated and discussed below. Four probe was used as a method of measurement by analyzing the resistance of the samples under microscope. The samples were placed on a glass substrate with a double sided tape and placed under the microscope for analyzes. The results below were obtained from the reading on the Four probe microscope.

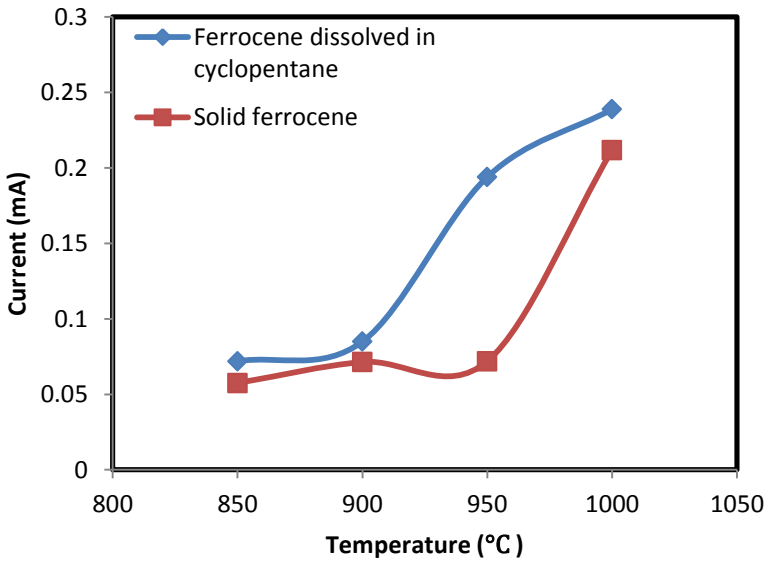

Figure 2: Electrical conductivity of the synthesized CNTs

A direct proportional relationship occurs between the reaction temperature and the current emitted for both CNTs produced with solid ferrocene and the dissolved ferrocene in

cyclopentane. The increase in the electrical conductivity with increasing temperatures is mainly because CNTs have high number of Sp^2 bonds at high temperatures thus improving the field emissions and the electron transport of CNTs (Igbokwe et al., 2019). It is also evident from the graph that the samples produced with liquid catalyst obtained the highest current (mA) when compared to solid catalyst due to increased hydrocarbon concentration in the reaction resulting in formation of single-walled CNTs (Awasthi et al., 2005). The maximum current achieved when Ferrocene was dissolved in cyclopentane is $0.2388\ mA$ whereas the maximum current obtained when using solid catalyst is $0.2117\ mA$.

4.4. Results and Discussion for CNT yarn

4.4.1.SEM images produced at reactor temperatures between $900 - 1000^0C$

From Figure 24, CNT yarn produced with 160 ml/min are more aligned than the CNT yarn produced at 150 ml/min. Both SEM images for Figures 24(a) and 24(b) show impurities in the CNT yarns produced. CNT yarns produced at 950 ℃ for both methane flow rates show less impurities as compared to CNT yarns produced at 900 and 1000℃. The high catalyst impurities at reaction temperature of 1000 ℃ are attributed by the agglomeration and deactivation of metal particles at very high temperatures (Ming et al., 2016). This leads to bigger particles of metal catalyst as illustrated by Figure 26(b). Impurities at 900 ℃ could be due to the deactivation of catalyst due to low temperature in the reactor and the accumulation of amorphous carbon.

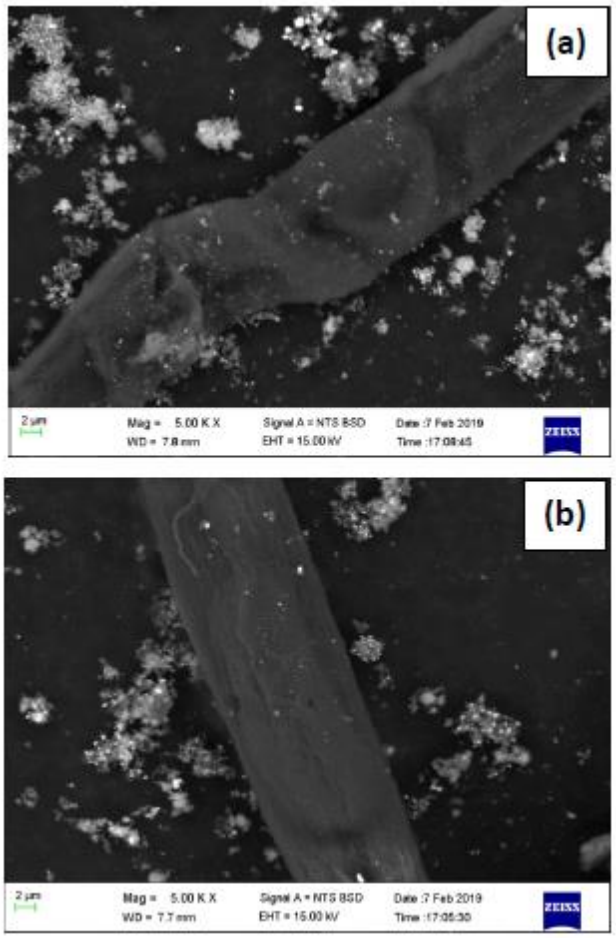

Figure 3: SEM images produced at **900** ℃ (a) Methane flow rate at 150 ml/min (b) Methane flow rate at 160 ml/min

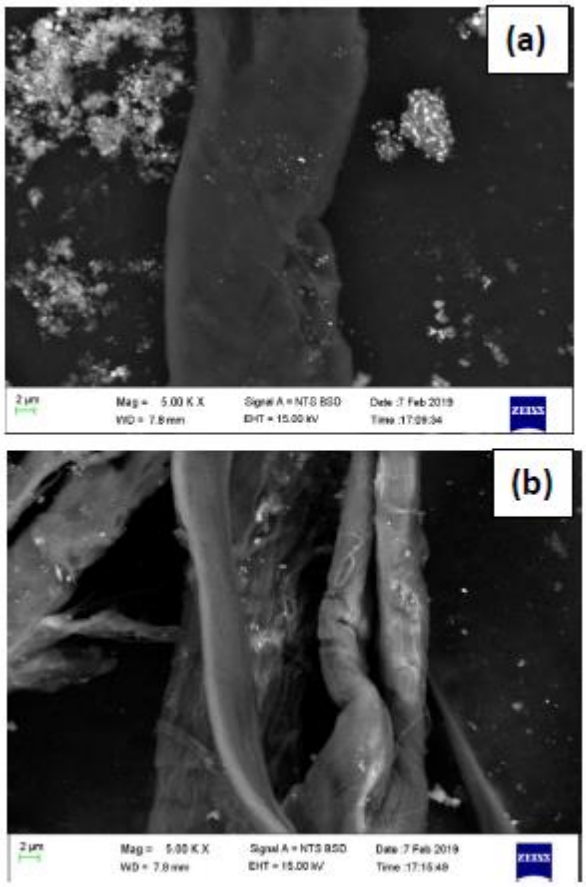

Figure 4: SEM images produced at **950** ℃ (a) Methane flow rate at 150 ml/min (b) Methane flow rate at 160 ml/min

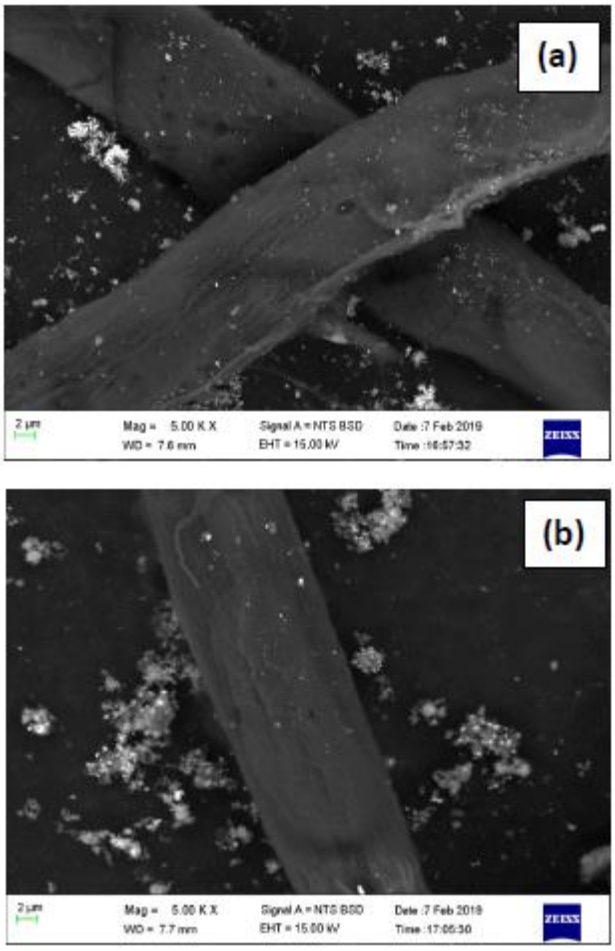

Figure 5: SEM images produced at 1000 ℃ (a) Methane flow rate at 150 ml/min (b) Methane flow rate at 160 ml/min

4.4.2. Effect of temperature and methane flow rate on CNT yarn yield

The CNT yarn yield increased at high temperatures and high methane flow rates. This follows the same analogy that the reactor temperature is directly proportional to the growth rate and average diameter (Lee et al., 2001). The increase of CNT yarn yield with increasing methane flow rate is again due to the prolonged precursor resident time on the catalyst surface which then increases the decomposition rate of carbon into the catalyst (Tee et al., 2009). As a result, more CNT yarn growth occurs.

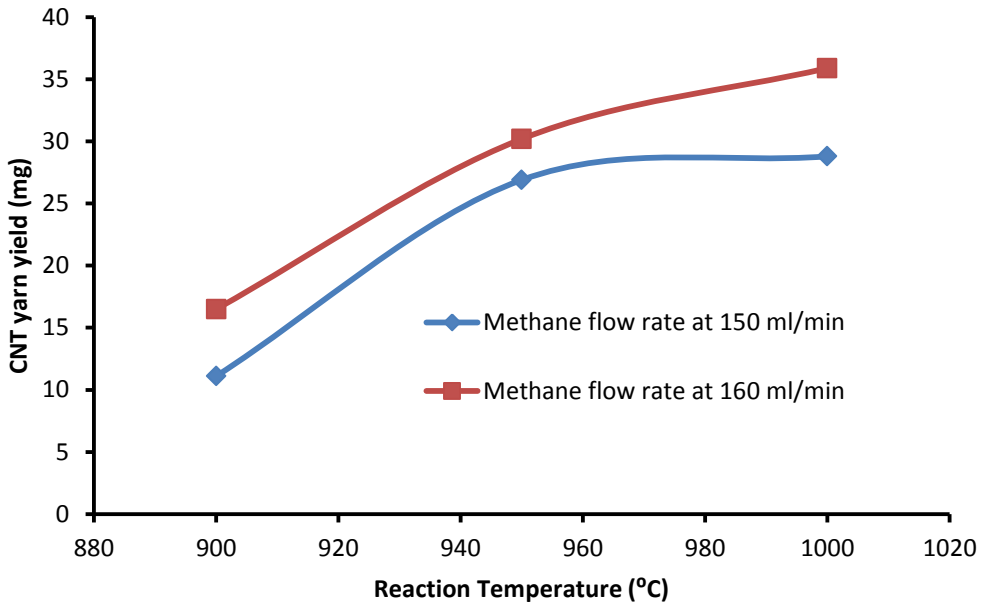

Figure 6: The effect of temperature and methane flow rate on CNT yarn yield

4.4.3. Raman Spectroscopy Results

From the spectra it is visible that there is a mixture of both single-walled and multi-walled yarns because Radial Breathing Modes (RBM) were found at lower wavenumbers and the G-band has a shoulder on the left due to G+-G- splitting from the curvature of the graphite sheet in the nanotube.

The ratio of the intensities of D and G bands was used as a measure of the quality of the bulk samples. This was done to determine the degree of defect for the samples. Table 5 below contains the I_G/I_D ratios for the CNT yarn samples where the peak area of the D band was obtained at Raman shift of $1350\ cm^{-1}$ and the peak area of the G band was obtained at Raman shift of $1582\ cm^{-1}$.

The sample's I_D/I_G ratios decrease with the increasing reaction temperature. This means that G-band intensity becomes stronger at increasing reaction temperatures (Ming et al., 2016). This could be due to the same reason as formation of CNTs that are straight and longer CNTs are likely to form at higher temperatures attributed by the alterations in the distribution of atoms at the metal/gas interface thus giving more pure samples (Atieh et al., 2012). Furthermore, high

reaction temperatures promote the surface decomposition of hydrocarbons instead of hydrogenation reactions (Atieh et al., 2012). The reaction flow rate also has an effect on the I_D/I_G ratio since the ratio increases with increasing methane flow rate. It is evident that at higher flow rates the CNT yarns formed have higher I_D/I_G ratios therefore it means the purity of CNT yarns at 150ml/min is better than at 160 ml/min. This observation could be due the fact that at high methane flow rates the decomposition of carbon occurs faster than the diffusion of carbon. Therefore excess carbon gets absorbed onto the catalyst surface leading to the catalyst deactivation (Ming et al., 2016).

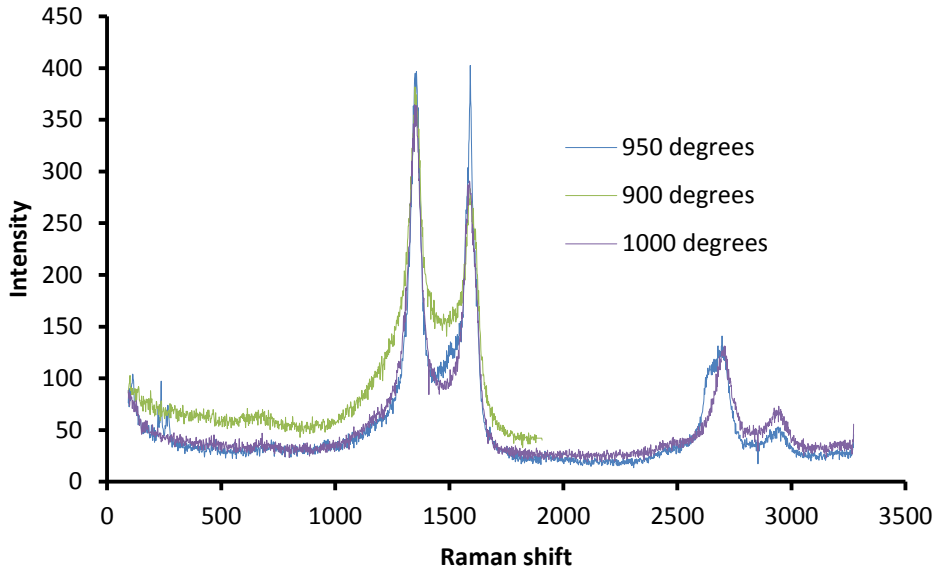

Figure 7: Raman results for CNT yarn produced at various temperatures with methane flow rate of 150 ml/min

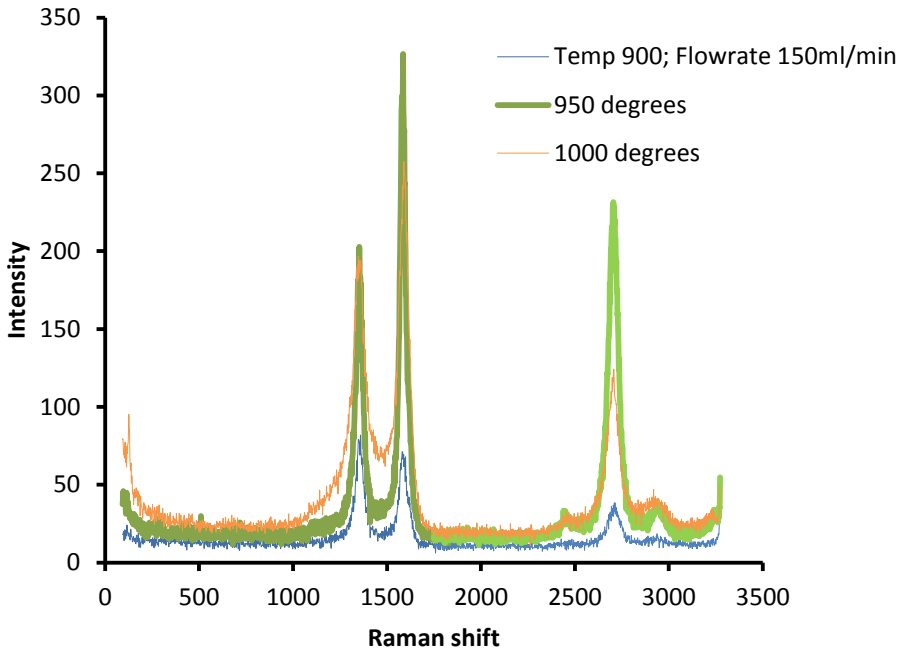

Figure 8: Raman results for CNT yarn produced at various temperatures with methane flow rate of 160 ml/min

Table 5: I_D/I_G ratios for CNT yarns produced at various temperatures and methane flow rates

Reaction temperature (°C)	**I_D/I_G ratio**	**Methane flow rate (ml/min)**
900	2.09	160
950	1.19	160
1000	1.27	160
900	1.09	150
950	0.79	150
1000	0.64	150

4.4.4. Analysis by four-point probe

Similarly, with the CNT bundles the current emitted by the CNT yarn increases with the increasing temperature and this also could be due to the increasing Sp^2 bonds at high temperatures (Igbokwe et al., 2019). Moreover, high temperatures favour the synthesis of pure CNT yarn due to the alterations in the distribution of atoms at the gas-solid interface (Atieh et al., 2012). However the electrical conductivity of CNT yarns decreases with increasing methane flow rate and this could be the result of formation of amorphous carbon due to the increased carbon concentration in the reaction since high flow rates allows for longer residence time (Ming et al., 2016). The highest emitted current achieved is $0.2638\ mA$ produced at temperature of 1000 ℃ and flow rate of $150\ ml/min$.

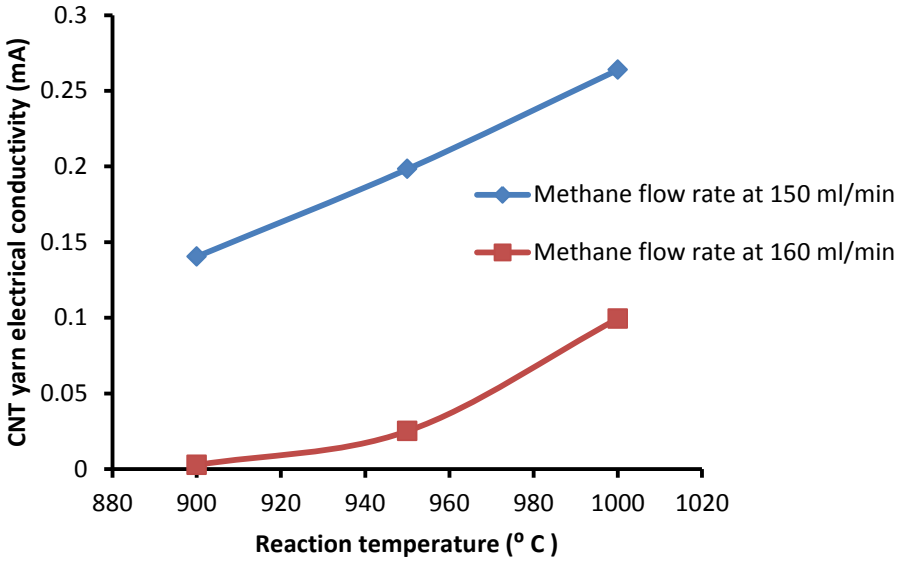

Figure 9: Electrical conductivity results for CNT yarns produced at various temperatures and methane flow rates

4.5. Concluding remark

From analysing the synthesized samples using SEM, Raman spectroscopy and Four-point probe techniques, it was found that CNTs manufactured with the dissolved ferrocene are better aligned and longer compared to using a solid catalyst. This could be due to the ability of liquid ferrocene to vaporize quickly and travel to the reactor faster than the solid ferrocene which had the tendency of crystallizing at the neck of the vaporizer. For CNT production, the highest yield was achieved at reactor temperature 950℃ using the dissolved ferrocene. The addition of more

carbons atoms from the cyclopentane used to dissolve ferrocene could be the reason for high CNT yields. Also with lower reaction temperatures the decomposition of carbon is slow whereas at high reaction temperatures promotes catalyst poisoning due to high amounts of amorphous carbon in the reaction environment. The latter could be the reason why the highest yield was realised at 950℃. The purity and electrical conductivity of the samples improved when the dissolved ferrocene was used at high reaction temperatures and this is attributed by the high number of sp^2 bonds found at high temperatures. For the synthesis of CNT yarn, the purity and electrical conductivity of the samples were found to be high when lower methane flow rates were used. This could be attributed by the increased flow in the reaction environment leading to carbon precursor being flashed too quick before nucleation of CNTs formed.

CHAPTER FIVE

5. Parametric effect of production variables and optimization

5.1. Introduction

RSM is a statistical approach employed for modelling and optimization of process parameters (Aydar et al., 2018). This study entails the simulation analysis of the production of CNT yarn by varying parameters such as reactor temperature, carbon precursor flow rate, catalyst state and spinning rate.

The design of experiments was done using RSM for the selected combinations of the varied parameters. A systematic approach that considered interaction between the selected parameters was of critical importance in order to obtain accurate results. Hence RSM from DOE was chosen to optimize the CNT and CNT yarn production parameters to evaluate the combined effect of input factors on output responses (Bratz, 2016). The results in this section were analysed in terms of highest yield and electrical conductivity

5.2. Experimental method

The parametric effect of CNT yarn was carried out using RSM with CCD for designing the experiment and optimization using the Design – Expert 12 software. The application of DoE allowed the evaluation of interactive effects of reaction temperature and methane flow rate on the responses. The DoE ran 9 experimental matrixes as indicated in Table 7. Table 6 contains the range and values of production variables at different levels (high and low).

Table 6: The operating variables with actual values and levels

Variable	Units	Low	High	-alpha	+alpha
Temperature	℃	900	1000	879.289	1020.710
Methane flow rate	ml/min	150	160	147.929	162.071

Table 7: Experimental matrices from CCD

Experimental runs	Factor 1: A (Temperature)	Factor 2: B (Methane flow rate)
1	900	150
2	1000	150
3	900	160
4	1000	160
5	950	150
6	950	150
7	950	160
8	900	150
9	1000	160

The actual values for both factor 1 and factor 2 indicated in Table 7 were accomplished by the use of a CCVD reactor depicted in Section 3. Detailed laboratory experimental method can be obtained from Section 3 as well. The experiment was performed by varying the factors as indicated in Table 6.

5.3. Results and discussion

5.3.1. Parametric effect on CNT yarn yield

This section employed RSM to explain the main and interactive effects of the studied variables (temperature and methane flow rate) on the CNT yarn yield and the electrical conductivity.

A linear model was suggested by the CCD design to predict the values for yield. The predicted equation for the CNT yield is shown in Equation 1 below. Table 7 shows the actual and predicted experimental values from the laboratory and from DoE.

Table 8: Comparison of actual and predicted experimental results using the linear model

Run Order	Actual Value	Predicted Value	Leverage	Internally Studentized Residuals	Externally Studentized Residuals	Influence on Fitted Value DFFITS	Standard Order
1	11.00	14.78	0.459	-1.546	-1.820	-1.678	1
2	28.00	24.38	0.261	1.266	1.350	0.803	8
3	16.00	16.86	0.351	-0.323	-0.297	-0.219	3
4	28.00	29.81	0.315	-0.657	-0.623	-0.423	2
5	26.00	22.30	0.207	1.249	1.326	0.678	7
6	16.00	16.86	0.351	-0.323	-0.297	-0.219	5
7	30.00	31.89	0.532	-0.830	-0.806	-0.858	4
8	28.00	29.81	0.315	-0.657	-0.623	-0.423	6
9	26.00	22.30	0.207	1.249	1.326	0.678	9

$$\boldsymbol{Yield = -151.68 + 0.150A + 0.208B} \qquad \text{Equation 1}$$

From Table 9, the analysis of variance was conducted through ANOVA test on the developed model. The p-value of 0.0052 indicated the significance of the model terms since it was less than 0.0500. Temperature (A) in this case is a significant model term. This is because values greater than 0.1000 indicate model terms are not significant thus making methane flow rate insignificant. The Model F-value of 14.31 indicates the model is significant with 0.52% chance that an F-value this large occurs due to noise (Sarrai et al., 2016).

Based on the model R^2 of 0.827 indicated in Table 10, means that 82.7% of the results in the case of yield were explained. Since the R^2 is larger than 0.75 it means the model has a high reliability

in predicting the CNT yarn yield. The predicted R^2 of 0.608 is in reasonable agreement with the adjusted R^2 of 0.769 because the difference is less than 0.2 (Illaiyaraja et al., 2015). Moreover, adequate precision of 8.90 indicates an adequate signal since it is greater than 4 (Montgomery, 2001).

Table 9: Analysis of variance for CNT yield predicted model

Source	**Sum of Squares**	**d_f**	**Mean Square**	**F-value**	**p-value**	
Model	317.07	2	158.53	14.31	0.0052	significant
A-Temperature	313.31	1	313.31	28.27	0.0018	
B-Methane flow rate	8.90	1	8.90	0.8034	0.4046	
Residual	66.49	6	11.08			
Lack of Fit	66.49	3	22.16			
Pure Error	0.00	3	0.00			
Cor Total	383.56	8				

Table 10: Correlation Coefficient

Std. Dev.	3.33	R^2	0.8267
Mean	23.22	Adjusted R^2	0.7689
C.V. %	14.33	Predicted R^2	0.6076
		Adequate Precision	8.9017

The model graphs were plotted to visualize the effect of process parameters on yield. Contour and 3-D surface plots were further used to determine the optimization of the yield. From Figure 31, the experimental data is spread around the modelled curve indicating a good correlation between the predicted and experimental data. Figure 32 and Figure 33 indicates that yield is sensitively affected by the temperature more than the methane flow rate. A small increase in

reactor temperature causes a huge increase in CNT yarn yield as compared to the methane flow rate. This is mainly attributed by the increased sp2 bonds at high temperatures resulting to the increased CNT yarn yield (Igbokwe et al., 2019). Also the insignificance of methane flow rate on the yield could be due to the increased decomposition rate of carbon as compared to it diffusion rate onto the catalyst (Atieh et al., 2012). The observations seen from Figure 32 and 33 validates the findings in Section 4 illustrated in Figure 27 since the effect of methane flow rate was small as compared to the temperature effect on CNT yarn yield.

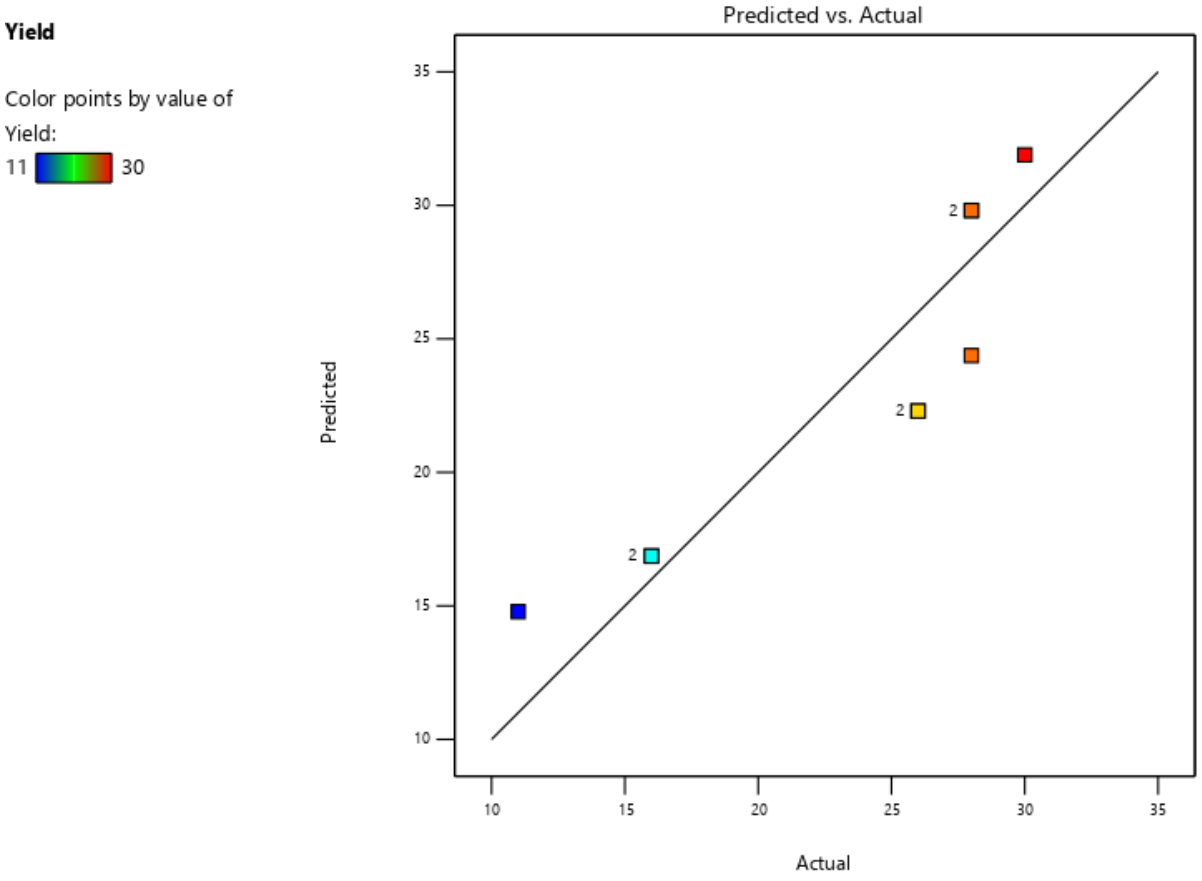

Figure 10: The actual and predicted experimental results for CNT yield

The Figure 32 illustrates the contour of CNT yarn yield while varying temperature and methane flow rate.

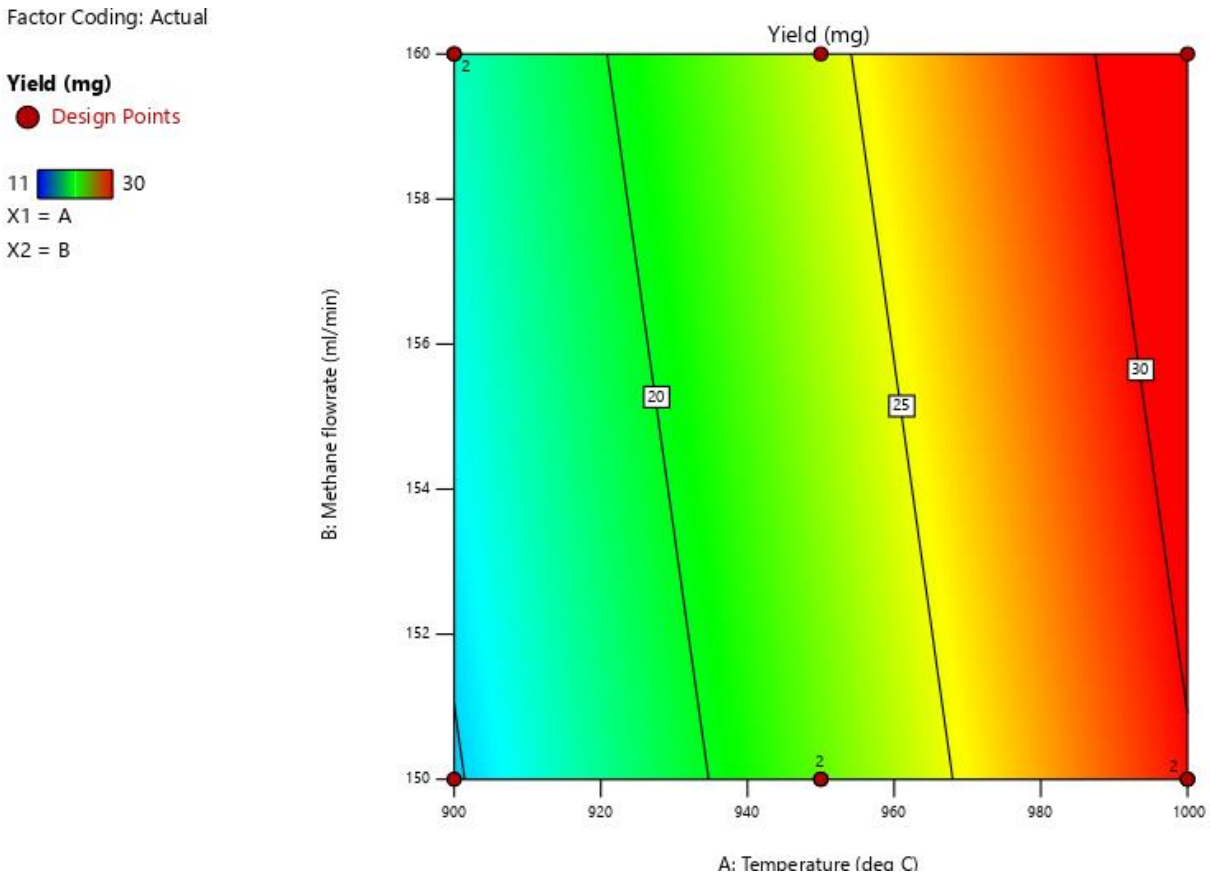

Figure 11: A contour for CNT yarn yield at various operating parameters

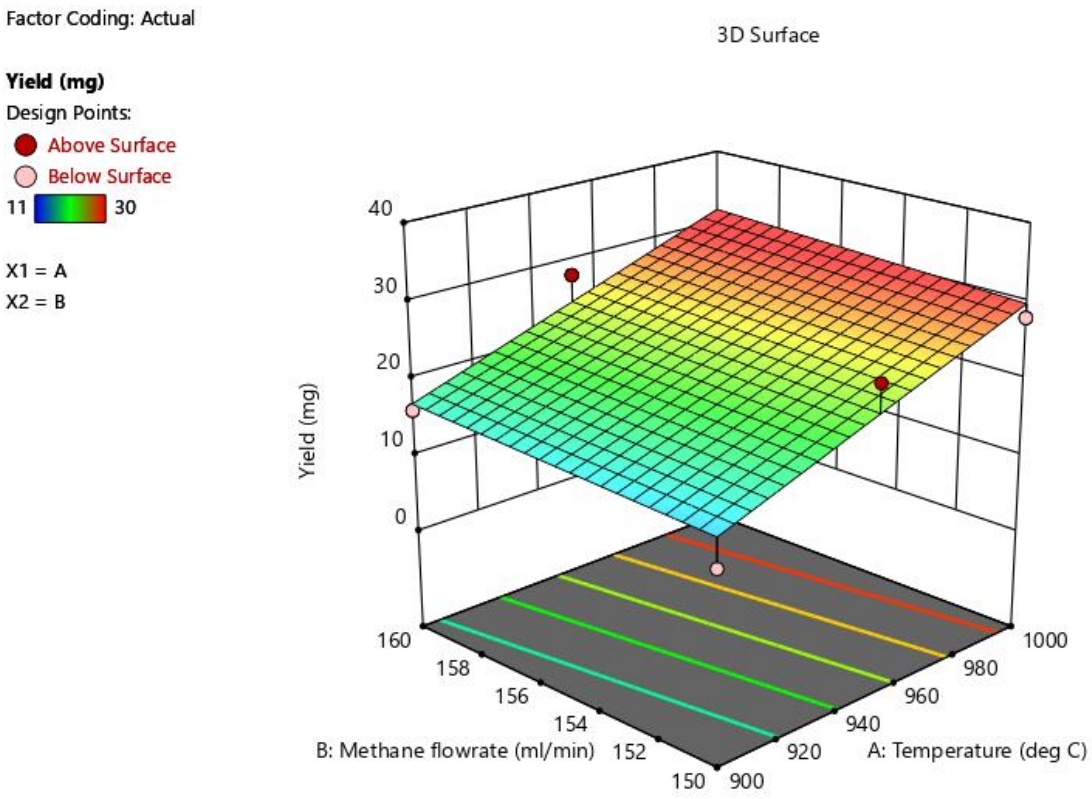

Figure 12: A three-dimensional surface plot for CNT yarn yield

5.3.2. Parametric effect on CNT yarn electrical conductivity

The similar method was followed for analysing the electrical conductivity of CNT yarn depending on the reactor temperature and methane flow rate. Table 11 shows the actual and predicted experimental values using the suggested linear model. The predicted model equation for the electrical conductivity is highlighted in Equation 2.

Table 11: The actual and predicted values for electrical conductivity by varying parameters

Run Order	Actual Value	Predicted Value	Leverage	Internally Studentized Residuals	Externally Studentized Residuals	Influence on Fitted Value DFFITS	Standard Order
1	140.00	151.62	0.459	-1.004	-1.005	-0.927	1
2	25.00	51.16	0.261	-1.934	-2.875	-1.710	8
3	15.00	0.5135	0.351	1.143	1.179	0.868	3
4	26.00	252.92	0.315	0.774	0.745	0.505	2
5	198.00	202.27	0.207	-0.305	-0.280	-0.143	7
6	15.00	0.5135	0.351	1.143	1.179	0.868	5
7	99.00	101.81	0.532	-0.261	-0.240	-0.255	4
8	263.00	252.92	0.315	0.774	0.745	0.505	6
9	198.00	202.27	0.207	-0.305	-0.280	-0.143	9

$$\boldsymbol{Y2 = 1506.58 + 1.01A - 15.11B} \qquad \textbf{Equation 2}$$

ANOVA test was used to examine the accuracy/significance of the predicted model. The model F-value of 164.32 implies that the model is significant with only a 0.01% chance that an F-value this big could be due to noise. For the CNT yarn electrical conductivity, both the temperature (A) and methane flow rate (B) are significant model terms with p-values less than 0.0500. From Table 13 below the model has correlation coefficient (R^2) of 0.982 which indicates a high reliability of the model in predicting the electrical conductivity of the CNT yarn. This further means that 98.2% of the data variation can be explained by the suggested model. The predicted R^2 of 0.969 is in reasonable agreement with the adjusted R^2 of 0.981 since the difference is less than 0.2. The adequate ratio of 31.32 indicates an adequate signal of the model since it is higher than 4 (Owolabi et al., 2018). The results from ANOVA are indicated in Table 12.

Table 12: Analysis of variance for electrical conductivity of CNT yarn

Source	Sum of Squares	d_f	Mean Square	F-value	p-value	
Model	81440.02	2	40720.01	164.32	< 0.0001	significant
A-Temperature	14237.34	1	14237.34	57.45	0.0003	
B-Methane flowrate	46935.86	1	46935.86	189.40	< 0.0001	
Residual	1486.86	6	247.81			
Lack of Fit	1486.86	3	495.62			
Pure Error	0.0000	3	0.0000			
Cor Total	82926.89	8				

Table 13: Correlation Coefficient for CNT yarn electrical conductivity

Std. Dev.	15.74	R^2	0.9821
Mean	135.11	Adjusted R^2	0.9761
C.V. %	11.65	Predicted R^2	0.9609
		Adequate Precision	27.7715

The model graphs for the better illustration of the influence of temperature (A) and methane flow rate (B) on the electrical conductivity are plotted in Figure 34. The experimental data plotted in Figure 34 forms a straight line on top of the predicted curve which indicates a strong correlation between the experimental and predicted data. From both Figure 35 and Figure 36 shows that the reactor temperature (A) and methane flow rate (B) changes the electrical conductivity of the CNT yarn sensitively. Similarly to the trends observed in Section 4.4.4, the electrical conductivity increases with increasing reactor temperature and decreasing methane flow rate. This is attributed by the promotion of SWCNTs formation at high temperatures due to the high catalyst activity compared to lower temperatures (Toussi et al., 2011). SWCNTs possess good electrical conductivity property compared to MWCNTs (Behabtu et al., 2008). The high carbon source flow rate enables longer residence time which allows the accumulation of carbon atoms in

the reaction thus limiting the diffusion rate of carbon leading to catalyst poising. Therefore amorphous carbon forms as a resultant of catalyst poising then reducing the quality of CNTs (Ming et al., 2016).

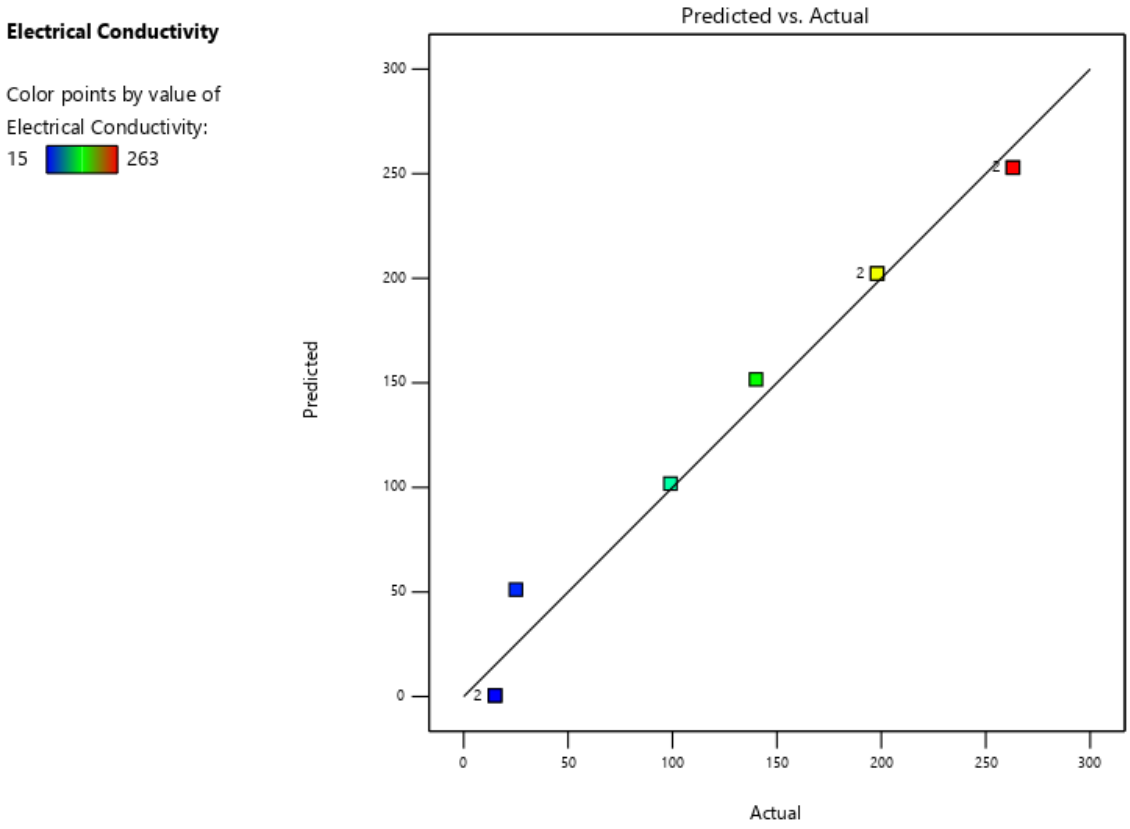

Figure 13: A scatter plot for predicted value and actual experimental value for electrical conductivity

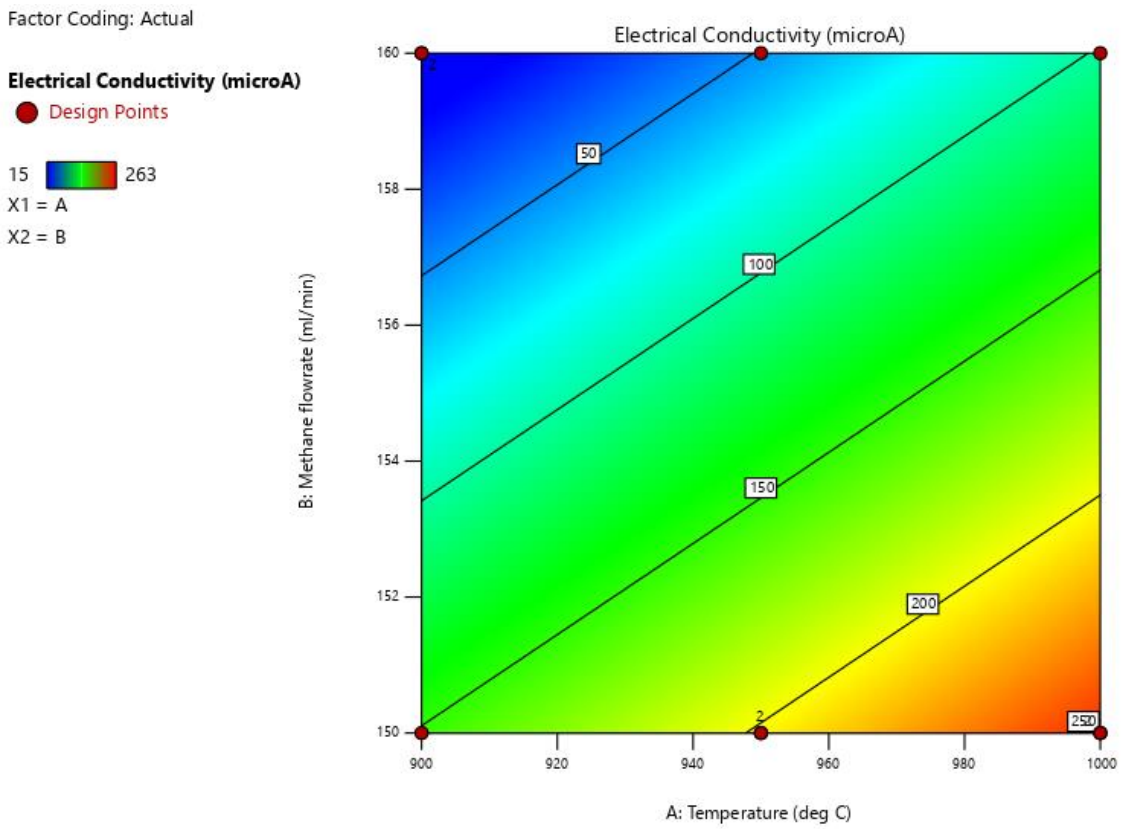

Figure 14: An illustration of contour for electrical conductivity with the effect of temperature and methane

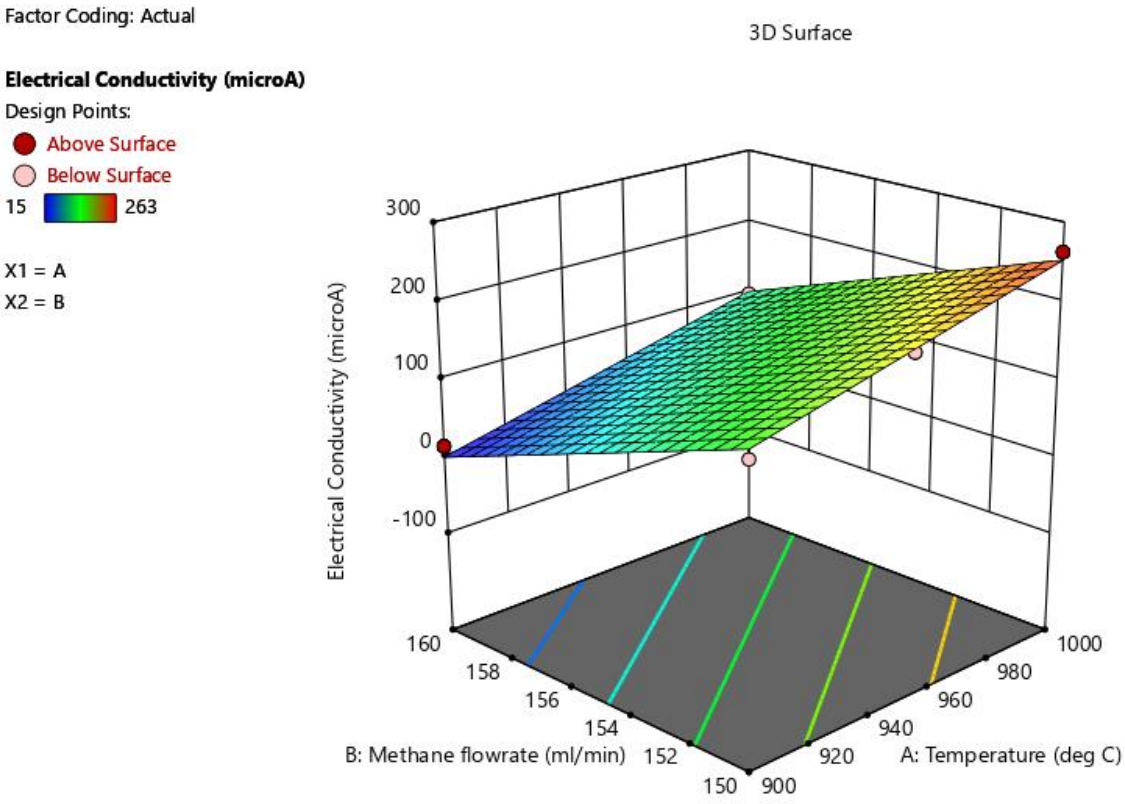

Figure 15: A 3-D surface plot for electrical conductivity

After modelling of the experimental data, the optimization values for the study were determined and illustrated in Figure 37(a), 37(b) and 37 (c) below. The predicted optimal values for the yield and electrical conductivity are 24.72 mg and 0.217 mA, respectively. These optimum responses occurs at the reactor temperature of 967 ℃ and methane flow rate of 150 ml/min.

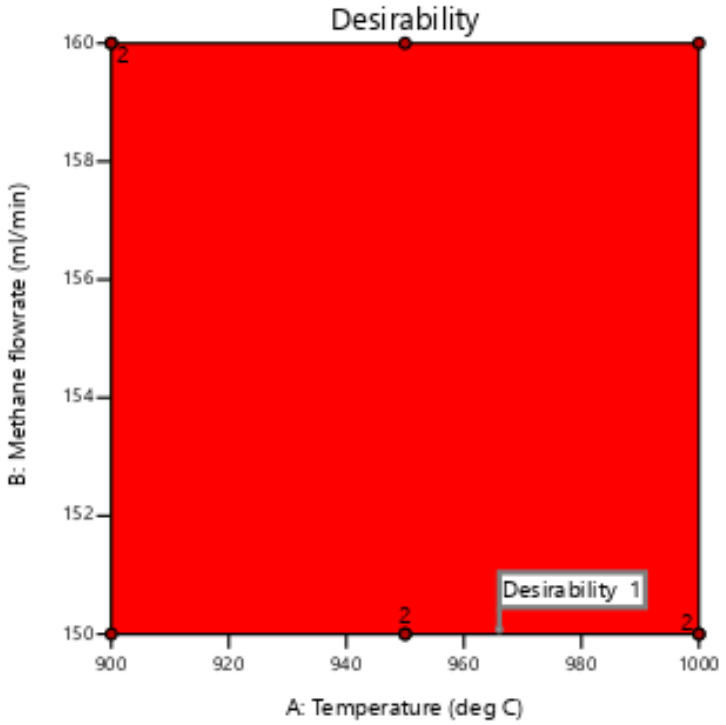

Figure 16 (a): CNT yarn optimized results for desirable production parameters

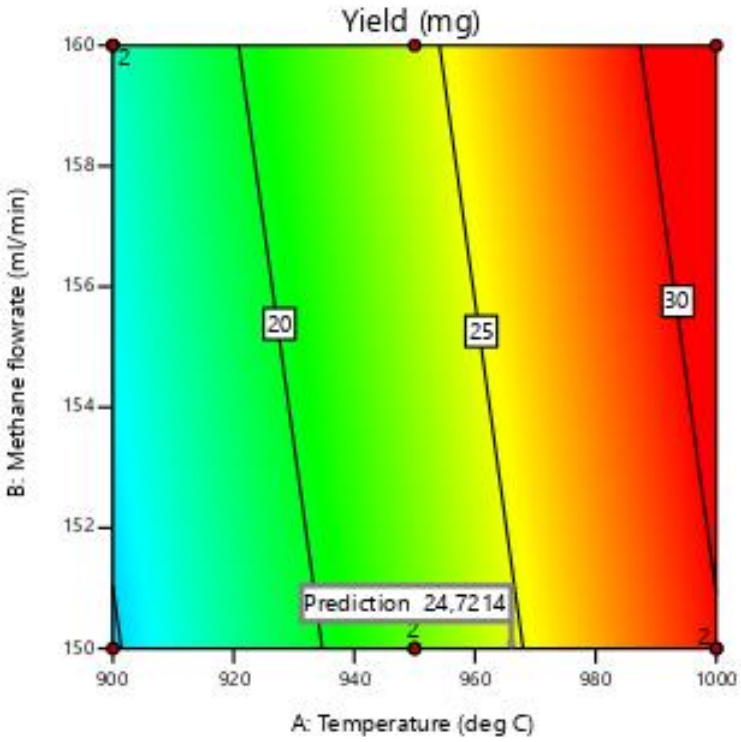

Figure 17(b): Predicted optimum yield of CNT yarn

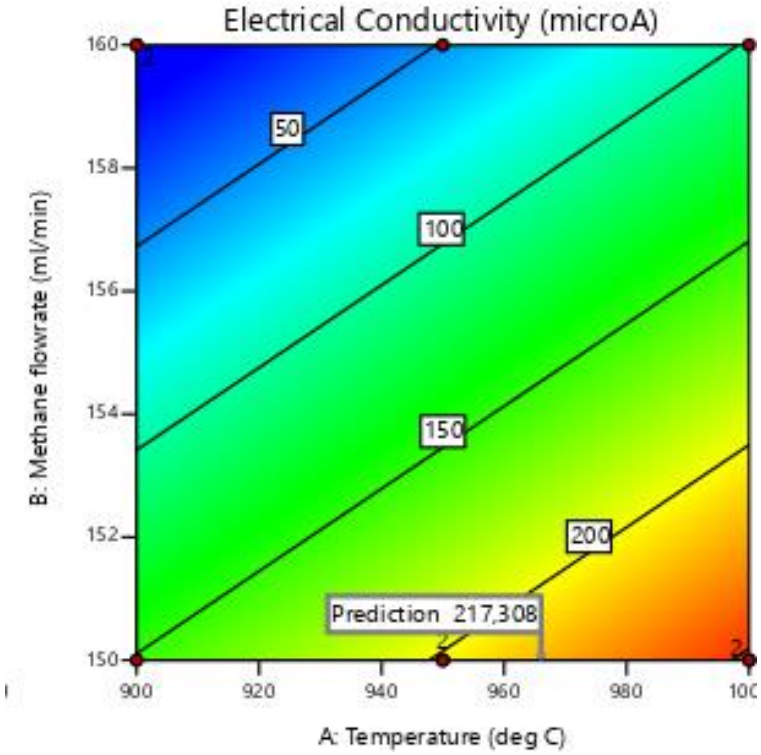

Figure 18 (c): Predicted optimum electrical conductivity of CNT yarn

CHAPTER SIX

6. Conclusion and recommendations

6.1. Conclusions

From the production, characterization and optimization of the CNTs, SEM images have shown the formation of more straight and aligned CNTs when ferrocene was dissolved in cyclopentane. Results from Raman have indicated fewer defects in the CNTs produced with the dissolved ferrocene when compared to CNTs synthesized with solid ferrocene based on the I_D/I_G ratios of their intensities. When the catalyst state was changed by dissolving Ferrocene in cyclopentane; the quality of the CNTs improved. Cyclopentane has also proved to increase the CNT yield. Moreover, the optimal CNT yield was obtained at $1000\,℃$ with liquid ferrocene solution having 165mg, 0.2388mA and 0.16 yield, electrical conductivity and I_D/I_G ratio, respectively. From characterizing the CNT samples it was observed that the yield, electrical conductivity and purity increases at high temperature. Moreover, dissolving catalyst in cyclopentane improves the purity, yield and the electrical conductivity of CNTs which could be due to the increased saturated hydrocarbons in the reaction.

Similarly with the CNTs, CNT yarn was formed, characterized and optimized. The variables during CNT yarn were the carbon source flow rate and reaction temperature. The optimal CNT was produce at 1000ºC with methane flow rate of 152 ml/min. This sample had 36.29 mg, 0.22 mA and 0.906, yield, electrical conductivity and I_D/I_G ratio, respectively. Similarly, with CNTs, the purity and electrical conductivity of CNT yarn improve with high temperature. However, increasing methane flow rate decrease the purity and the electrical conductivity of the CNT yarn which could be from the formations of amorphous carbon as a result of increasing carbon concentration.

From the optimization study of the CNT yarn, the optimal conditions were found at reactor temperature of $967\,℃$ and methane flow rate of $150\,mg$. These conditions would yield CNT yarn with mass of 24.72 mg and the electrical conductivity of 0.217 mA.

6.2. Recommendations

It is recommended for future work that other hydrocarbons such as Xylene be used as solvents for the Ferrocene catalyst. This would be a way of checking the effect of liquid hydrocarbons on the solid catalyst. Furthermore, purification methods should be considered and investigate the degree of defects before and after purification. Reaction temperature ranges above 1000ºC should be studied together with the effect of spinning rate on the properties of CNT yarn. Other optimization techniques such as Box-Benhken should be used to investigate the effect of parameters on CNT yarn production.

REFERENCES

Aberefa, S., Bedasie, K., Madhi, S., & Daramola, M. (2018). Production of carbon nanotube yarn from swirled floating catalyst chemical vapour deposition: a preliminary study. *Advances in Natural Sciences: Nanoscience and Nanotechnology*, 9, 1-8. https://doi.org/10.1088/2043-6254/aad5cb

Amri, A., Zulfansyah., Fermi, M., Sulistyati, I., Suryani, A., & Hambali, E. (2008). Modeling variables influence and optimization using response surface method – central composite design (rsm-ccd) on the sodium lignosulfonate production from palm oil stem biomass. *Jurnal Sains dan Teknologi*, 1-6.

Aqel, A., El-Nour, K., Amma, R., & Al-Warthan, A. (2012). Carbon nanotubes science and technology part (I) structure synthesis and characterization. *Arabian J. Chem.* 5, 1-23. doi:10.1016/j.arabjc.2010.08.022.

Awasthi, K., Srivastava, A., & Srivastava, O. (2005). Synthesis of carbon nanotubes. *J. Nanoscience and Nanotechnology*, 1-66.

Atieh, M., Guan, C., Fakhru-Razi, A., & Mahdi, E. (2012). Effect of reaction temperature on the production of carbon nanotubes. *Nano: Brief and Reports Review*, 1(3), 251-257. doi.org/10.1142/S1793292006000288.

Aydar, A. (2018). Utilization of response surface methodology in optimization of extraction of plant materials, *Intechopen*, 158 -169. http://dx.doi.org/10.5772/intechopen.73690

Behabtu, N., Green, J., & Pasquali, M. (2008). Carbon nanotube based neat fibers. *Nanotoday*, 3(5), 24 -34. https://doi.org/10.1016/S1748-0132(08)70062-8

Bell, M., Teo, K., Lacerda, R., Milne, W., Hash, D., & Meyyappan, M. (2006). Carbon nanotubes by plasma-enhanced chemical vapour deposition. *Pure & Applied Chem.* 78(6), 1117-1125. doi:10.1351/pac200678061117.

Beyerlein, I., Porwal, P., Zhu, Y., Xu, F., & Phoenix, L. (2009). Probabilistic strength of carbon nanotubes. *Solid Mechanics & Its Strength*, 1-13. doi:10.1007/978-90-481-3467.

Chen, G., Futaba, D., & Hata, K. (2017). Catalysts for the growth of carbon nanotube forest and superaligned arrays. *MRS Bulletin*, 42, 802-808. https://doi.org/10.1557/mrs.2017.235

Choo, H., Jung, Y., Jeong, Y., Kim, H., & Ku, B. (2012). Fabrication and application of carbon nanotube fibers. *Carbon Letters*, 13(4), 191 – 204. http://dx.doi.org/10.5714/CL.2012.13.4.191

Chrzanowska, J., Hoffman, J., Malolepszy, A., Mazurkiewicz, M., Kowalewski, T., Szymanski, Z., & Stobinski, L. (2015). Synthesis of carbon nanotubes by the laser ablation method: Effect of laser wavelength. *Basic Solid State Physics,* 252(8), 1860-1867. https://doi.org/10.1002/pssb.201451614

Coleman, J., Khan, U., Blau, W., & Gun'ko, Y. (2006). Small but strong: A review of the mechanical properties of carbon nanotubes-polymer composites. *Carbon*, 44(9), 1624-1652. https://doi.org/10.1016/j.carbon.2006.02.038

Dahmen, K. (2003). Chemical vapour deposition. *Encyclopaedia of Physical Science and Technology*, 3, 787-808. https://doi.org/10.1016/B0-12-227410-5/00102-2

Danafar, F., Fakhru'l-Raz, A., Salleh, M., & Biak, D. (2009). Fluidized bed catalytic chemical vapour deposition synthesis of carbon nanotubes – A review. *Chem. Eng. J.*, 155, 37 – 48. doi:10.1016/j.cej.2009.07.052

De Volder, M., Tawfick, S., Baughman, R., & Hart, J. (2013). Carbon nanotubes: Present and future commercial applications. *Science*, 535 – 539. Doi:10.1126/science.1222453

Eatemadi, A., Daree, H., Kaimkhanloo, H., Kouhi, M., Zarghami, N., Akbarzadeh, A.,Joo, S. (2014). Carbon nanotube properties, synthesis, purification and medical applications. *Nanoscale Research Letters*, 9 (1), 393. doi:10.1186/1556-276X-9-393

Ghemes, A., Muramatsu, J., Minami, Y., Okada, M., Inoue, Y., & Mimura, H. (2012). High performance carbon nanotube fiberspun from long multiwalled carbon nanotubes. *J. Adv. Res. Phy.*, 1-3.

Hamedani, Y., Macha, P., Bunning, T., Naik, R., & Vasudev, M. (2015). *Plasma-enhanced chemical vapour deposition: Where we are and the outlook for the future*. IntechOpen. doi:10.5772/64654.

Hayashi, Y., Iijima, T., Suzuki, T., Kimoshita, H., Oshima, H., & Tokunaga, T. (2015). Improved properties of carbon nanotube yarn spun from dense and long carbon nanotube forest.

Paper presented at the International Conference on Manipulation, Manufacturing and Measurement on the Nanoscale, Changchun.

Hirsch, A., & Vostrowsky, O. (2005). *Functionalization of carbon nanotubes: Functional molecular nanostructures. Topics in Current Chemistry.* Springer. https://doi.org/10.1007/b98169.

Hiura, H., Ebbesen, T., Tanigaki, K. (1995). Opening and purification of carbon nanotubes in high yields. *Advanced Materials*, 7(3), 275 – 276. https://doi.org/10.1002/adma.19950070304

Hou, P., Liu, C., & Cheng, M. (2008). Purification of carbon nanotubes. *Carbon*, 46(15), 2003 – 2005. doi:10.1016/j.carbon.2008.09.009.

Howarth, R., Santoro, R., & Ingraffea, A. (2011). Methane and the greenhouse gas footprint of natural gas from shale formations. *Climate Change*, 1 – 12. doi:10.1007/s10584-011-0061-5.

Huang, Y., & Terentjev, E. (2012). Dispersion of carbon nanotubes: Mixing, sonication, stabilization and composite properties. *Polymers*, 4, 275 – 295. doi:10.3390/polym4010275.

Hwang, S., Park, Y., Yoon, K., & Bang, D. (2011). Smat material structures based on carbon nanotube composite. *Intechopen*, 371 – 396. http://doi.org/10.5772/17374.

Illaiyaraja, N., Likith, K., Babu, G., & Khanum, F. (2015). Optimization of extraction of bioactive compounds from feronia limonia (wood apple) fruit using response surface methodology (RSM). *Food Chemistry*, 173, 348-354.

Ismail, A., Goh, P., Tee, J., & Aziz, M. (2008). A review of purification techniques for carbon nanotubes. *Nano Brief Reports and Reviews*, 3(3), 127-143. doi:10.1142/S1793292008000927

Jayashinge, C., Amstutz, T., Schulz, M., & Shanov. (2013). Improved processing of carbon nanotubes. *Journal of Nanomaterials*, 1-7. http://dx.doi.org/10.1155/2013/309617

Jiang, K., Wang, J., Li, Q., Liu, L., C., & Fan, S. (2011). Superaligned carbon nanotubes arrays, films and yarns: A road to applications. *Advanced Materials*, 1154-1161. https://doi.org/10.1002/adma.201003989

Jurmann, G., & Tammeveski, K. (2006). Electroreduction of oxygen on multiwalled carbon nanotubes modified highly oriented pyrolytic graphite electrodes in alkaline solutions. *Journal of Electroanalytical Chemistry*, 597(2), 119-126. doi 10.1016/j.jelechem.2006.09.002

Khavarian, M., Chai, S., Tan, S., & Mohamed, R. (2013). Effects of growth parameters on morphology of aligned carbon nanotubes synthesized by floating catalyst and the growth model. *Fullerene, Nanotubes, and Carbon Nanostructures*, 21 (9), 765-777. doi:10.1080/1536383X.2012.654544

Lekawa-Raus, A., Patmore, J., Kurzepa, L., Bulmer, J., & Koziol, K. (2014). Electrical properties of carbon nanotube based fibers and their future use in electrical wiring: Advanced Functional Materials. *Materials*, 24, 3661 – 3682. doi:10.1002/adfm.201303716

Liu, K., Sun, Y., Zhou, R., Wang, J., Liu, L., Fan, S., & Jiang, K. (2010). Carbon nanotube yarn with high tensile strength made by twisting and shrinking method. *J. Engineered Fibers and Fabrics*, 1-7. doi:10.1088/0957-4484/21/4/045708

Liu, W., Xu, F., Zhu, N., & Wang, S. (2006). Mechanical and electrical properties of carbon nanotubes. *Journal of Engineered Fibers and Fabrics*, 11(4), 36-41

Luo, X., Weng, W., Liang, Y., Hu, Z., Zhang, Y., Yhang, J., … Cheng, H. (2019). Multifuctional fabrics of carbon nanotube fibers. *J. Materials Chem. A*, 7(15), 8790 – 8797. doi:10.1039/C9TA01474H

Mahalingam, P., Parasuram, B., Maiyalagan, T., & Sundaram, S. (2012). Chemilcal methods for purification of carbon nanotubes – A review. *J. Environmental Nanotechnology*, 1(1), 53 – 65

Makris, D., Giorgi, L., Giorgi, R., Lisi, N., & Salernitano, E. (2005). CNT growth on alumina supported nickel catalyst by thermal CVD. *Diamonds and Related Materials*, 14, 815 – 819. doi:10.1016/j.diamond.2004.11.001

Medjo, R. (2013). Characterization of carbon nanotubes. *Intech Open Science*, 162 – 183. http://dx.doi.org/10.5772/51540

Miao, M. (Ed). (2020). Carbon nanotube fibers and yarns for smart textiles: Production, properties and applications in smart textiles. Elsevier.

Ming, H., Peiling, D., Yunlong, Z., Jing, G., & Xiaoxue, R. (2016). Effect of reaction temperature on carbon yield and morphology of CNTs on copper loaded nickel nanoparticles, *J. Nanomaterials*, 1 – 5. http://dx.doi.org/10.1155/2016/8106845

Montgomery, D. (2001). Design and analysis of experiments. New York, USA: John Wiley & Sons.

Mourdikoudis, S., & Thanh, N. (2018). Characterization techniques for nanoparticles: Comparison and complementarity upon studying nanoparticle properties. *Nanoscale*, 12871 – 12934. https://doi.org/10.1039/C8NR02278J

Ovejero, G., Sotelo, J., Romero, M., Rodriguez, A., Ocana, M., Rodriguez, G., & Garcia, J. (2006). Multiwalled carbon nanotubes for liquid-phase oxidation: Functionalization, characterization and catalytic activity. *Industrial & Engineering Chemistry Research*, 45(7), 2206 -2212. doi: 10.1021/ie051079p

Owolabi, R., Usman, M., & Kehinde, A. (2018). Modelling and optimization of process variables for the solution polymerization of styrene using response surface methodology. *J. King of Saudi University*, 30, 22-30. http://dx.doi.org/10.1016/j.jksues.2015.12.005

Pandey, P., & Dahiya, M. (2016). Carbon nanotubes: Types, methods of preparation and applications. *Int. J. Pharmaceutical Science and Research*, 1(4), 15 – 21.

Panth, A. (2008). Functional properties of nanomaterials. *Carbon Nanotube*, 1 – 15

Rafique, M., & Igbal, J. (2011). Production of carbon nanotubes by differnt routes: A review. *Journal of Encapsulation and Absorption Scinces*, 1(2), 29-34. doi:10.4236/jeas.2011.11004

Rajamani, D., Ziout, A., Balasubramanian, E., Velu, R., Sachin, S., & Mohamed, H. (2018). Prediction and analysis of surface roughness in selective inhibition sintered high-density polyethyleneparts: A parametric approach usingresponse surface methodology–greyrelational analysis. *Advances in Mechanical Engineering*, 10(12), 1-16. doi: 10.1177/1687814018820994

Rashid, H., Yu, K., Naveed, U., Anjum, M., Khan, A., Ahmad, N., & Jan, M. (2015). Catalyst role in chemical vapor deposition (CVD) process: A review. *Reviews on Advanced Materials Science*, 40(3), 235 – 248.

Schumacher, J. (nd). Carbon nanotube growth using plasma enhanced chemical vapour deposition. [Word]. Retrieved from http://rsl.eng.usf.edu/Documents/Tutorials/TutorialsCNTGrowth.pdf

Scoville, C., Cole, R., Hogg, J., Farooque, O., & Rusell, A. (n.d). Carbon nanotube. [Pdf] Retrieved from https://courses.cs.washington.edu

Sengupta, J., & Jacob, C. (2010). The effect of Fe and Ni catalysts on the growth, J. Nanoparticle Research, 12, 457-465.

Sharma, R., Sharma, A., & Sharma, V. (2015). Synthesis of carbon nanotubes by arc-discharge and chemical vapor deposition method with analysis of its morphology, dispersion and functionalization characteristics. *Cogent Engineering*, 2(1),1-10. https://doi.org/10.1080/23311916.2015.1094017

Speltini, A., Merli, D., Quartarone, E., & Profumo, A. (2010). Separation of alkanes and aromatic compounds by packed column gas chromatography using functionalized multiwalled carbon nanotubes as stationary phases. *J. Chromatography A*, 1217(17), 2918 – 2924. https://doi.org/10.1016/j.chroma.2010.02.052

Szabo, A., Perri, C., Csato, A., Giordang, G., Vuono, D., & Nagy, J. (2010). Synthesis methods of carbon nanotubes and related materials. *Materials*, 3092-3140. doi:10.3390/ma3053092

Tee, J., Ismail, A., & Aziz, M. (2009). Effect of reaction temperature and flow rate of precursor on formation of multi-walled carbon nanotubes. *Jurnal Teknoligi*, 49, 141 -147, https://doi.org/10.1063/1.3160133

Toussi, S., L-Razi, A., Chuah, A., & Suraya, A. (2011). Effect of synthesis condition on the growth of SWCNTs via catalytic chemical vapour deposition. *Sains Malaysiana*, 40(3), 197-201.

Tran, C., Lucas, S., Phillips, D., Randeniya, L., Baughman, R., & Tran-cong, T. (2011). Manufacturing polymer/carbon nanotube composite using a novel direct process. *Nanotechnology*, 22(14), 145302. Doi:10.1088/0957-4484/22/14/145302.

Vilatela, J., & Windle, A. (2012). A multifunctional yarn made of carbon Nanotubes. *J. Engineered Fibers and Fabrics*, 7(3), 23-28. doi:10.1177/155892501200702S04.

Wang, X., Yong, Z., Li, Q., Bradford, P., Liu, W., & Tucker, D. (2013). Ultrastrong, stiff and multifunctional carbon nanotube composites. *Materials Research Letters*, 1(1), 19-25.https://doi.org/10.1080/21663831.2012.686586.

Wang, Y., Wei, F., & Gu, G. (2002). Agglomerated carbon nanotubes and its mass production in a fluidized-bed reactor. *Physica B: Condensed Matter*, 323(1-4), 327-329.doi:10.1016/S0921-4526(02)01041-4.

Wei, J., Zhu, H., Wu, D., & Wei, B. (2004). Carbon nanotube filaments in household lightbulbs. *Applied Physiscs Letters*, 84(24), 4869-4871.doi:10.1063/1.1762697.

Wepasnick, A., Smith, A., Bitter, J., & Fairbrother, D. (2009). Chemical and structural characterization of carbon. *Anal Bioanal Chem*, 1-12. doi: 10.1007/s00216-009-3332-5

Yaosef, S., & Mohamed, A. (2016). Mass production of CNTs using CVD multi-quartz tubes. *Journal of Mechanical Science and Technology*, 5135-5141.

Zhang, X., et al. (2007). Strong carbon nanotube fibers spun from long carbon nanotube arrays. *Small*, 3(2), 244-248.https://doi.org/10.1002/smll.200600368.

Zhang, J., Jiang, D., & Peng, H., A (2013) pressurized filtration technique for fabricating carbon nanotube buck paper: Structure, mechanical and conductive properties. *Micropor. Mesopor. Mater.*, 184(15), 127-133. https://doi.org/10.1016/j.micromeso.2013.10.012.

7. Appendices

7.1. Optimization Data

7.1.1. The Fit summary for yield

Source	Sequential p-value	Lack of Fit p-value	Adjusted R^2	Predicted R^2	
Linear	**0.0052**		**0.7689**	**0.6076**	**Suggested**
2FI	0.9713		0.7227	0.0474	
Quadratic	< 0.0001		0.9948	0.9446	Aliased

7.1.2. Model summary statistics for yield

Source	Std. Dev.	R^2	Adjusted R^2	Predicted R^2	PRESS	
Linear	**3.33**	**0.8267**	**0.7689**	**0.6076**	**150.51**	**Suggested**
2FI	3.65	0.8267	0.7227	0.0474	365.37	
Quadratic	0.5000	0.9974	0.9948	0.9446	21.24	Aliased

7.1.3. The fit summary for electrical conductivity

Source	Sequential p-value	Adjusted R^2	Predicted R^2	
Linear	**< 0.0001**	**0.9761**	**0.9609**	**Suggested**
2FI	0.0800	0.9854	0.9347	
Quadratic	0.1037	0.9913	0.9075	Aliased

7.1.4. Model summary statistics for electrical conductivity

Source	Std. Dev.	R^2	Adjusted R^2	Predicted R^2	PRESS	
Linear	**15.74**	**0.9821**	**0.9761**	**0.9609**	**3241.60**	**Suggested**

2FI	12.32	0.9909	0.9854	0.9347	5415.64	
Quadratic	9.50	0.9956	0.9913	0.9075	7669.06	Aliased